



Mechanism of Viral Glycoprotein Targeting by Membrane-Associated RING-CH Proteins

Cheng Man Lun,^a Abdul A. Waheed,^a Ahlam Majadly,^a Nicole Powell,^a Eric O. Freed^a

^aVirus-Cell Interaction Section, HIV Dynamics and Replication Program, Center for Cancer Research, National Cancer Institute, Frederick, Maryland, USA

ABSTRACT An emerging class of cellular inhibitory proteins has been identified that targets viral glycoproteins. These include the membrane-associated RING-CH (MARCH) family of E3 ubiquitin ligases that, among other functions, downregulate cell surface proteins involved in adaptive immunity. The RING-CH domain of MARCH proteins is thought to function by catalyzing the ubiquitination of the cytoplasmic tails (CTs) of target proteins, leading to their degradation. MARCH proteins have recently been reported to target retroviral envelope glycoproteins (Env) and vesicular stomatitis virus G glycoprotein (VSV-G). However, the mechanism of antiviral activity remains poorly defined. Here we show that MARCH8 antagonizes the full-length forms of HIV-1 Env, VSV-G, Ebola virus glycoprotein (EboV-GP), and the spike (S) protein of severe acute respiratory syndrome coronavirus 2 (SARS-CoV-2), thereby impairing the infectivity of virions pseudotyped with these viral glycoproteins. This MARCH8-mediated targeting of viral glycoproteins requires the E3 ubiquitin ligase activity of the RING-CH domain. We observe that MARCH8 protein antagonism of VSV-G is CT dependent. In contrast, MARCH8-mediated targeting of HIV-1 Env, EboV-GP, and SARS-CoV-2 S protein by MARCH8 does not require the CT, suggesting a novel mechanism of MARCH-mediated antagonism of these viral glycoproteins. Confocal microscopy data demonstrate that MARCH8 traps the viral glycoproteins in an intracellular compartment. We observe that the endogenous expression of *MARCH8* in several relevant human cell types is rapidly inducible by type I interferon. These results help to inform the mechanism by which MARCH proteins exert their antiviral activity and provide insights into the role of cellular inhibitory factors in antagonizing the biogenesis, trafficking, and virion incorporation of viral glycoproteins.

IMPORTANCE Viral envelope glycoproteins are an important structural component on the surfaces of enveloped viruses that direct virus binding and entry and also serve as targets for the host adaptive immune response. In this study, we investigate the mechanism of action of the MARCH family of cellular proteins that disrupt the trafficking and virion incorporation of viral glycoproteins across several virus families. This research provides novel insights into how host cell factors antagonize viral replication, perhaps opening new avenues for therapeutic intervention in the replication of a diverse group of highly pathogenic enveloped viruses.

KEYWORDS E3 ubiquitin ligase, viral glycoproteins, HIV-1 Env, VSV-G, Ebola virus GP, SARS-CoV-2 spike protein, cellular inhibitory factors

Viruses rely heavily on host cellular machinery to replicate due to their relatively limited coding capacity. In turn, cells have evolved extensive and elaborate defense mechanisms to impede virus replication. Cells carry genes that encode numerous proteins, often referred to as inhibitory or restriction factors, that are central components of the innate immune response that serves as the first line of defense against invading pathogens. Well-characterized restriction factors include apolipoprotein B mRNA editing catalytic polypeptide-like (APOBEC) family proteins, tripartite motif protein 5 α (TRIM5 α), SAM and HD domain-containing protein 1 (SAMHD1), Myxovirus resistance 2

Citation Lun CM, Waheed AA, Majadly A, Powell N, Freed EO. 2021. Mechanism of viral glycoprotein targeting by membrane-associated RING-CH proteins. *mBio* 12:e00219-21. <https://doi.org/10.1128/mBio.00219-21>.

Editor Stephen P. Goff, Columbia University/HHMI

This is a work of the U.S. Government and is not subject to copyright protection in the United States. Foreign copyrights may apply.

Address correspondence to Eric O. Freed, efreed@nih.gov.

This article is a direct contribution from Eric O. Freed, a Fellow of the American Academy of Microbiology, who arranged for and secured reviews by Chen Liang, Lady Davis Institute, and Marc C. Johnson, University of Missouri, School of Medicine.

Received 27 January 2021

Accepted 28 January 2021

Published 16 March 2021

(Mx2), and tetherin/BST-2 (1). These restriction factors are either expressed constitutively and/or are induced by interferon (IFN) (2–4). Recently, an emerging class of host proteins have been shown to specifically target the synthesis, trafficking, and/or function(s) of viral glycoproteins (5). These include the IFN-induced transmembrane (IFITM) proteins, guanylate-binding proteins (GBPs), endoplasmic reticulum class I α -mannosidase (ERManI), galectin 3-binding protein (LGALS3BP/90K), Ser incorporator (SERINC), and the MARCH proteins (5–13).

Viral envelope glycoproteins, which are important structural components decorating the surfaces of enveloped virus particles, recognize receptors on target cells and mediate viral entry by catalyzing membrane fusion events either at the plasma membrane or in low-pH endosomes following endocytic uptake of the viral particle. They are synthesized and cotranslationally glycosylated in the endoplasmic reticulum (ER) and then traffic through the secretory pathway to the site of virus assembly (14). During trafficking through the Golgi apparatus, some viral glycoproteins are cleaved by furin or furin-like proteases as a requisite step in the generation of the fusion-active viral glycoprotein complex. Viral glycoproteins often multimerize (e.g., as trimers) during trafficking (14). Many enveloped viruses assemble at the plasma membrane, whereas some assemble in alternative compartments. For example, SARS-CoV-2 particles are thought to assemble in the ER/Golgi intermediate compartment (ERGIC) and be released by exploiting lysosomal organelles (15, 16).

Ubiquitin is a small, 76-amino-acid protein that is highly expressed in eukaryotic cells. It can be attached to target proteins, usually on Lys residues, but occasionally on Ser, Thr, or Cys residues, via a multienzyme cascade involving an E1 ubiquitin-activating enzyme, an E2 ubiquitin-conjugating enzyme, and an E3 ubiquitin ligase (17). Ubiquitin attachment can serve as a signal for target protein degradation in the proteasome or lysosome, or it can regulate the endocytic trafficking of the target protein or other aspects of protein function.

The membrane-associated RING-CH (MARCH) family of RING-finger E3 ubiquitin ligases comprise 11 structurally diverse members. With the exception of the cytosolic MARCH7 and MARCH10 proteins, MARCH family members are transmembrane proteins containing multiple (ranging from 2 to 14) putative membrane-spanning domains and bearing an N-terminal cytoplasmic RING-CH domain (Fig. 1) (18). MARCH proteins were originally discovered as cellular homologs of the K3 and K5 E3 ubiquitin ligases of Kaposi's sarcoma-associated herpesvirus (KSHV) (19, 20). These viral MARCH protein homologs confer escape from the host immune response by downregulating the major histocompatibility complex class I (MHC-I) antigen on the surfaces of virus-infected cells (21, 22). Other large DNA viruses encode analogous proteins involved in immune evasion (23). Cellular MARCH proteins have been reported to downregulate numerous proteins, including MHC-II (24), transferrin receptor (25), TRAIL receptors (26), CD44 and CD81 (27), interleukin 1 (IL-1) receptor accessory protein (28), CD98 (29), and tetherin/BST-2 (30). The RING-CH domain of MARCH proteins and its interaction with E2 enzymes are responsible for their E3 ligase activity; thus, mutations that either inactivate the catalytic center of the RING domain or prevent interaction with E2s abrogate MARCH protein activity (18, 25, 28). MARCH proteins and their viral homologs generally catalyze the transfer of ubiquitin to Lys residues in the CTs of their target proteins, leading to their degradation and/or altered trafficking (18, 19, 25, 31–34). However, the viral MARCH protein homologs K3 and K5 of KSHV have been reported to attach ubiquitin to Ser, Thr, and/or Cys residues (35–37).

MARCH8 was first identified in a genome-wide small interfering RNA (siRNA) screen as a potential HIV-1 restriction factor acting early in the virus replication cycle by an unknown mechanism (38). More recently, three MARCH proteins—MARCH1, -2, and -8—were reported to be late-acting restriction factors that target retroviral Env glycoproteins and vesicular stomatitis virus G glycoprotein (VSV-G), thereby impairing infectivity of HIV-1 virions bearing these viral glycoproteins (6, 8, 11). The endogenous expression of MARCH proteins differs among cell types, with higher expression of MARCH1, -2, and -8 observed in myeloid cells such as monocyte-derived macrophages (MDMs) and

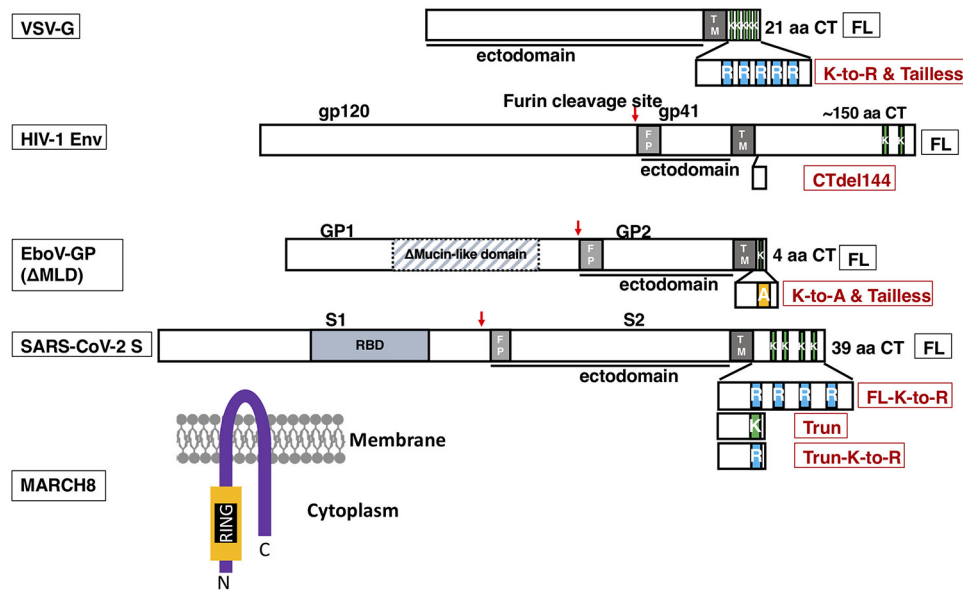


FIG 1 Organization of the viral envelope glycoproteins used in this study. Surface and transmembrane subunits of HIV-1 Env (gp120 and gp41), EboV-GP (GP1 and GP2), and SARS-CoV-2 S protein (S1 and S2) are indicated. Where appropriate, the site of furin cleavage is indicated by a red arrow. The Δ mucin-like domain (Δ MLD) (hatched rectangle outlined by a dashed line) and the receptor-binding domain (RBD) of the EboV-GP and SARS-CoV-2 S protein, respectively, are indicated. The fusion peptide (FP) and transmembrane domains (TM) are labeled. The length in amino acids (aa) of each full-length (FL) CT, and the number of Lys (K) residues in each CT, are indicated. Each CT mutant, and the Lys residues mutated to either Arg (R) or Ala (A), are shown. At the bottom is shown a schematic representation of the MARCH8 topology in the membrane, with two transmembrane domains and the RING finger E3 ligase domain. The structures of the viral glycoproteins and MARCH8 are not drawn to scale.

monocyte-derived dendritic cells (MDDCs) compared to primary CD4⁺ T cells (6, 11). MARCH8 expression has been reported to be particularly high in the lung (19). MARCH8 knockdown or knockout in myeloid cells increases HIV-1 infectivity, suggesting that MARCH8 may serve as an antiviral factor in these cell types (11). MARCH1, -2, and -8 are reported to be localized to lysosomes, endosomes, and the plasma membrane (18, 19, 25).

To understand the mechanism of MARCH-mediated antiviral activity in greater detail, envelope glycoproteins from four families of viruses were selected for study: the retrovirus HIV-1, the rhabdovirus VSV, the filovirus Ebola virus (EboV), and the coronavirus severe acute respiratory syndrome coronavirus 2 (SARS-CoV-2). Three of the glycoproteins encoded by these viruses (HIV-1 Env, EboV-GP, and SARS-CoV-2 spike [S] protein) are cleaved by furin, whereas VSV-G is not (39–41) (Fig. 1). HIV-1 Env is synthesized as a precursor, gp160, that is cleaved to gp120 and gp41; the EboV-GP precursor pre-GP is cleaved to GP1 and GP2, and the SARS-CoV-2 S protein precursor is cleaved to S1 and S2 (Fig. 1) (39–41). The cytoplasmic tails (CTs) of the viral glycoproteins investigated in this study are highly variable in length, with those of HIV-1 Env, SARS-CoV-2 S protein, VSV-G, and EboV-GP containing 150, 39, 21 and 4 amino acids, respectively (Fig. 1). These viral glycoproteins have CTs that vary not only in length but also in the number of Lys residues they contain, with two Lys residues in the CT of HIV-1 Env, four in the SARS-CoV-2 S protein, five in VSV-G, and one in the CT of EboV-GP (Fig. 1). These Lys residues could potentially serve as targets for MARCH-mediated ubiquitination. Our data demonstrate that each of the viral glycoproteins examined is antagonized, to variable extents, by MARCH8. We observed that MARCH-mediated inhibition of VSV-G is CT dependent, whereas inhibition of HIV-1 Env, EboV-GP, and SARS-CoV-2 S protein is CT independent. We further demonstrate that knockdown of endogenous *MARCH8* gene expression in HEK293T cells increases the infectivity of HIV-1 particles produced from those cells and that endogenous expression of

MARCH8 is induced by interferon (IFN) treatment in a human T-cell line, human peripheral blood mononuclear cells (hPBMCs), and primary human airway epithelial cells. Finally, we show that MARCH proteins colocalize with, and retain, the viral glycoproteins in an aberrant intracellular compartment that bears the lysosomal marker LAMP-1. Collectively, our data provide novel insights into the mechanism of action of the MARCH family of cellular E3 ubiquitin ligases and their ability to antagonize diverse viral envelope glycoproteins.

RESULTS

MARCH-mediated inhibition of viral envelope glycoproteins exhibits differential CT dependence. It has been shown that the ectopic expression of MARCH8 in virus producer cells markedly reduces the infectivity of HIV-1 virions bearing retroviral Env glycoproteins or VSV-G (6, 11). However, the molecular mechanism by which MARCH8 targets viral glycoproteins is not well defined. As mentioned in the introduction, it has been determined that MARCH proteins downregulate a number of proteins by transferring ubiquitin to their CTs, leading to their lysosomal degradation. To investigate the potential role of MARCH-mediated CT ubiquitination in the downregulation of viral glycoproteins, we deleted the CTs of HIV-1 Env, VSV-G, EboV-GP, and SARS-CoV-2 S protein (Fig. 1) and cotransfected the viral glycoprotein expression vectors with the Env(-) pNL4-3 derivative pNL4-3/KFS (42) or a luciferase-encoding NL4-3-derived vector virus. In the case of HIV-1, we used full-length pNL4-3 expressing wild-type (WT) Env or the CT-truncated Env mutant CTdel-144 (43). Virus-containing supernatants were harvested, normalized for p24 capsid content or reverse transcriptase (RT) activity, and used to infect the TZM-bl indicator cell line (44) or, in the case of the S protein pseudotypes, HEK293T cells stably expressing the human angiotensin-converting enzyme 2 (hACE2) receptor. Consistent with previous reports (6, 11), we observed that the infectivity of HIV-1 virions bearing VSV-G was markedly reduced (by ~10-fold) upon expression of WT MARCH8 in the virus producer cells (Fig. 2A). In contrast, the MARCH8-CS (25) and MARCH8-W114A (28, 45, 46) mutants, which abolish RING-CH function or interaction with E2 ubiquitin-conjugating enzyme, respectively, did not exert antiviral activity (Fig. 2A). We observed that the infectivity conferred by VSV-G Tailless was ~40% that of WT VSV-G, and overexpression of MARCH8 in virus producer cells had no significant effect on the infectivity of this VSV-G variant (Fig. 2A). Next, we investigated the ability of MARCH8 to inhibit a VSV-G mutant in which the Lys residues in the CT, which are potential sites of MARCH8-mediated ubiquitination, were substituted. A VSV-G mutant in which the five Lys residues in the CT were mutated to Ala displayed severely compromised infectivity (data not shown). We therefore introduced the more conservative Lys-to-Arg substitution (K-to-R) at these five Lys residues (Fig. 1) and observed that this mutant is fully infectious relative to the WT. As observed with the VSV-G Tailless mutant, overexpression of MARCH8 in virus producer cells had no significant effect on the infectivity of the VSV-G K-to-R mutant. As expected, the MARCH8 mutants likewise did not diminish the infectivity of either the Tailless or K-to-R VSV-G mutants. These results indicate that the ability of MARCH8 to antagonize VSV-G in this experimental system is dependent upon the Lys residues in the VSV-G CT, likely because they are targets of MARCH8-mediated ubiquitination.

As reported previously (6, 11), we observed that the infectivity of virus particles bearing HIV-1 Env is severely reduced (by ~10-fold) upon overexpression of WT MARCH8 in the virus producer cell. This inhibitory activity was to a large extent eliminated by the MARCH8-CS and MARCH8-W114A mutations (Fig. 2B). To investigate whether the inhibition of HIV-1 Env is CT dependent, we tested the CTdel144 Env mutant (43), which lacks nearly the entire gp41 CT (Fig. 1). Under these assay conditions, the infectivity of CTdel144 HIV-1 was ~40% that of WT HIV-1. Interestingly, in contrast to the lack of MARCH8-mediated inhibition observed with Tailless VSV-G, the infectivity of CT-deleted HIV-1 was reduced to a similar extent as the WT by expression of MARCH8 in the virus producer cells. The MARCH8 mutants did not significantly inhibit the infectivity of the CTdel144 HIV-1 Env mutant. These results demonstrate that MARCH8-mediated antagonism of HIV-1 Env requires the E3 ubiquitin ligase activity of the RING domain but does not require the gp41 CT.

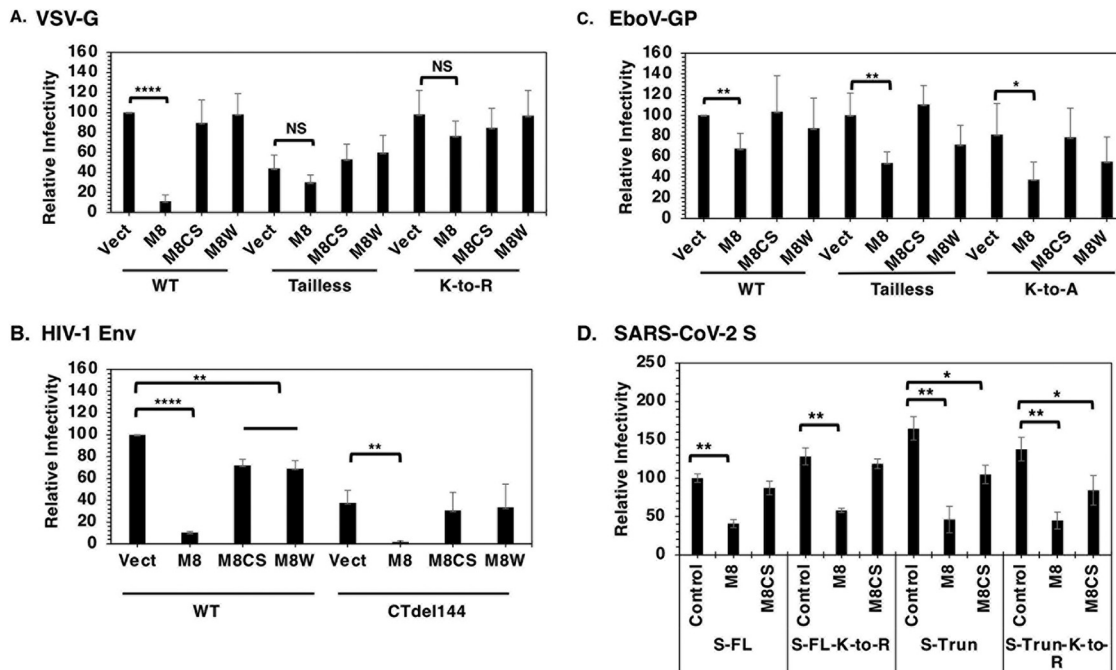


FIG 2 MARCH8-mediated targeting of viral envelope glycoproteins exhibits differential dependence on the CT. (A) HEK293T cells in a 12-well plate were cotransfected with the Env-defective HIV-1 molecular clone pNL4-3/KFS (1 μ g) and vectors expressing WT or mutant VSV-G (100 ng) and hemagglutinin (HA)-tagged WT or mutant MARCH8 (50 ng). TZM-bl cells were infected with VSV-G pseudotyped HIV-1, and luciferase activity was measured 2 days postinfection and normalized for viral p24. The infectivity of particles pseudotyped with WT VSV-G in the absence of MARCH8 is set at 100%. Abbreviations: Vect, vector; M8, MARCH8; M8CS, MARCH8-CS; MARCH8-W114A (M8W). (B) HEK293T cells were cotransfected with WT or CT-deleted (CTdel144) pNL4-3 HIV-1 molecular clones (1 μ g), and vectors expressing HA-tagged MARCH8 (WT or mutants) (100 ng). Two days posttransfection, virus supernatants were collected, analyzed for p24 content by western blotting, and infections were carried out in TZM-bl cells and normalized to p24 as described above for panel A. Infectivity of WT HIV-1 in the absence of MARCH8 was set at 100%. (C) HEK293T cells were cotransfected with Env-defective (pNL4-3/KFS) HIV-1 molecular clone (1 μ g) and vectors expressing EboV-GP (WT or CT mutants) (500 ng) and HA-tagged MARCH8 (WT or mutants) (250 ng), and infections were carried out in TZM-bl cells. The infectivity of particles pseudotyped with WT EboV-GP in the absence of MARCH8 was set at 100%. (D) HEK293T cells in a 6-well plate were cotransfected with the Env-defective, luciferase-expressing pNL4-3 derivative pNL4-3.Luc.R-E- (3 μ g) and vectors expressing SARS-CoV-2-S full-length (FL) and mutants (FL-K-to-R, Truncated, and Truncated-K-to-R) (300 ng) and HA-tagged MARCH8 (WT or CS mutant) (200 ng). Two days posttransfection, virus supernatant was collected, and infectivity was measured in HEK293T cells stably expressing hACE2 with RT-normalized virus. The infectivity of virus particles pseudotyped with full-length S protein (S-FL) in the absence of MARCH8 was set at 100%. Data shown are means plus standard deviations (SD) (error bars) from three to five independent experiments. Values that are significantly different by two-tailed unpaired *t* test are indicated by asterisks as follows: *, *P* < 0.05; **, *P* < 0.01; ****, *P* < 0.0001. Values that are not significantly different (NS) are also indicated.

As indicated above, the dependency on the CT for MARCH8-mediated inhibition differs between VSV-G and HIV-1 Env. We next examined the effect of MARCH8 on the infectivity of the EboV-GP, which contains a CT of only four amino acids (Fig. 1). For these experiments, we used a version of the EboV-GP lacking the mucin-like domain (47) as we obtained higher infectivity with this variant (data not shown). We will refer to this delta mucin-like domain variant (Δ MLD) as WT because it contains an intact CT. The infectivity of HIV-1 virions bearing either the WT or CT-deleted EboV-GP was reduced by ~30 to 40% when the virus was produced in the presence of MARCH8. We also mutated the single Lys residue in the CT of EboV-GP and observed that the infectivity of this K-to-A mutant was inhibited by ~50% in the presence of MARCH8. The infectivity of EboV-GP mutants was similar to that of the WT in the absence of MARCH8 overexpression (Fig. 2C). No statistically significant reduction in infectivity was observed for WT EboV-GP upon expression of the MARCH8-CS mutant, yet a minor reduction in infectivity was observed for EboV-GP Tailless and K-to-A mutants in the presence of the MARCH8-W114A mutant (Fig. 2C). These results demonstrate that MARCH8-mediated antagonism of EboV-GP is dependent on the E3 ubiquitin ligase activity of the RING domain but does not require the short EboV-GP CT.

We next tested the effect of MARCH8 overexpression on the infectivity of particles bearing the SARS-CoV-2 S protein, which has a 39-amino-acid CT with five Lys residues. We also tested a CT-truncated SARS-CoV-2 S protein, which bears a 19-amino-acid truncation and contains one Lys residue (Fig. 1). The infectivity of HIV-1 virions bearing WT or CT-truncated SARS-CoV-2 S protein was reduced by ~60% in the presence of MARCH8. We also mutated the Lys residues in the CTs of both WT and CT-truncated SARS-CoV-2 S proteins and observed ~50% reductions in particle infectivity upon overexpression of MARCH8 in the virus producer cell. The infectivity of particles bearing truncated or Lys-mutant SARS-CoV-2 S proteins was modestly higher than those bearing the WT S protein, likely due to disruption of the ER retention signal in the CT (48–50) (Fig. 2D). Expression of the inactive MARCH8-CS mutant did not reduce the infectivity of particles bearing the WT SARS-CoV-2 S protein or the full-length K-to-R mutant, but it did cause some reduction in the infectivity of virions bearing the CT-truncated forms of SARS-CoV-2 S protein (Fig. 2D).

We note that the effect of MARCH8 expression on the infectivity of particles bearing EboV-GP or SARS-CoV-2 S protein is modest relative to its effect on the infectivity of particles bearing VSV-G or HIV-1 Env. To investigate whether different levels of EboV-GP or SARS-CoV-2 S protein expression would affect the MARCH8-mediated inhibition of pseudotype infectivity, we performed transfections with a range of viral glycoprotein expression vector inputs. In the case of EboV-GP, we observed a 40 to 50% reduction in pseudotyped particle infectivity across the range of GP expression vector inputs (from 100 to 600 ng). In contrast, with SARS-CoV-2, we observed a fourfold reduction in infectivity with 100 ng input, but a more-modest twofold reduction with a 400-ng input (data not shown).

Altogether, the data presented in Fig. 2 demonstrate that MARCH8 overexpression in the virus producer cell inhibits the infectivity of virus particles bearing each of the four viral glycoproteins tested. The inhibitory activity of MARCH8 is largely abrogated by mutations reported to block E3 ubiquitin ligase activity (CS and W114A), although some residual inhibitory activity was observed with these mutants in some assays. Importantly, in the case of VSV-G, MARCH8-mediated inhibition is dependent on the Lys residues in the CT, whereas inhibition of HIV-1 Env, EboV-GP, and SARS-CoV-2 S protein does not require the CT.

MARCH8 expression in virus producer cells leads to viral envelope glycoprotein degradation and reduced processing and virion incorporation. To investigate the mechanism by which MARCH8 expression reduces the infectivity of virus particles bearing VSV-G, we transfected 293T cells with the Env(-) pNL4-3 molecular clone pNL4-3/KFS and the WT or mutant VSV-G expression vectors, with or without MARCH8 expression vectors. VSV-G levels in cell and virion fractions were quantified by western blotting (WB). Cotransfection with an expression vector for FLAG-tagged small glutamine-rich tetratricopeptide repeat-containing protein (SGTA) provided a loading control. As shown in Fig. 3A, overexpression of WT MARCH8 markedly reduced (by ~3-fold) the expression of VSV-G in both cell and virion fractions. Consistent with the lack of inhibition observed with the MARCH8-CS and MARCH8-W114A mutants in the infectivity assays (Fig. 2), significant reductions in VSV-G levels were not observed with these MARCH8 mutants (Fig. 3A and B) despite comparable WT and mutant MARCH8 expression levels (Fig. 3A). Also consistent with the infectivity data, overexpression of WT or mutant MARCH8 did not significantly affect levels of Tailless or K-to-R VSV-G mutants in either cell or virus fractions. We also observed that overexpression of MARCH8 had no significant effect on the expression of viral Gag proteins in cells or on virus release, which, together with the observed lack of effect on SGTA expression levels, indicated that the reduction of VSV-G levels in the presence of MARCH8 is not due to cytotoxicity or globally reduced protein expression. Finally, we observed a more rapid mobility of VSV-G in the presence of WT but not mutant MARCH8, presumably due to reduced VSV-G glycosylation induced by MARCH8 expression (Fig. 3A). This effect on VSV-G mobility was not observed with the Tailless or K-to-R mutants, consistent with these mutants being resistant to MARCH8-mediated inhibition.

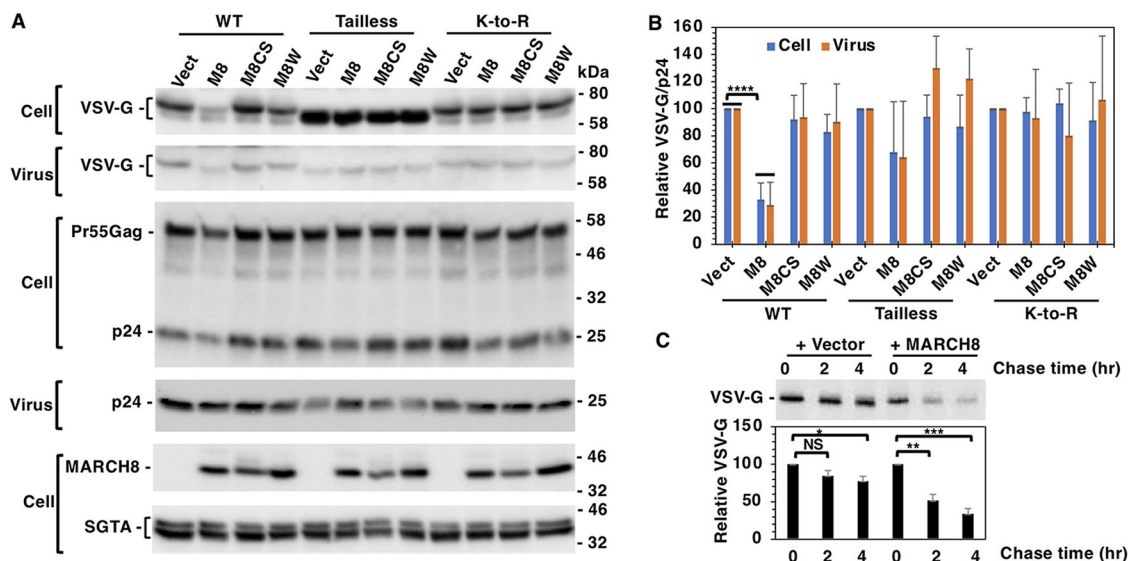


FIG 3 Effect of MARCH8 (M8) on virion incorporation of VSV-G is CT dependent. (A) HEK293T cells were cotransfected with the Env-defective HIV-1 molecular clone pNL4-3/KFS (1 μ g) and vectors expressing WT or mutant VSV-G (100 ng), HA-tagged WT or mutant MARCH8 (50 ng), and FLAG-tagged SGTA (200 ng) as a transfection control. Cell and viral lysates were prepared and subjected to western blot analysis with anti-VSV-G to detect VSV-G, HIV-Ig to detect the Gag proteins Pr55Gag and p24 (CA), anti-HA to detect HA-tagged MARCH8, or anti-FLAG to detect FLAG-tagged SGTA. The mobility of molecular mass standards is shown to the right of each blot. (B) The levels of VSV-G in cell and virus were quantified, and the levels of VSV-G in virus were normalized to viral p24. The levels of VSV-G in the absence of MARCH8 were set at 100%. (C) HEK293T cells were transfected with VSV-G expression vector in the presence (+) or absence of HA-tagged MARCH8 expression vector. One day posttransfection, cells were labeled with [³⁵S]Met/Cys for 20 min and then chased for 0, 2, or 4 h in unlabeled medium. Cell lysates were prepared, immunoprecipitated with anti-VSV-G antibody (Ab), and analyzed by SDS-PAGE followed by fluorography. The levels of VSV-G were quantified and set at 100% at time zero. Data shown are means plus SD from four or five (B) or two (C) independent experiments. Statistical significance (two-tailed unpaired *t* test): *, *P* < 0.05; **, *P* < 0.02; ***, *P* < 0.01; ****, *P* < 0.0001; NS, not significant.

To measure the half-life of VSV-G in the presence or absence of MARCH8, we performed pulse-chase analysis. 293T cells expressing WT VSV-G alone or coexpressing VSV-G with MARCH8 were pulse-labeled with [³⁵S]Met/Cys for 20 min and chased for 0, 2, or 4 h in unlabeled medium. We observed that MARCH8 overexpression reduced the levels of VSV-G, on average, to 52% and 34% at 2 and 4 h, respectively, compared to 85% and 78% in the absence of MARCH8 at those time points (Fig. 3C). These results indicate that MARCH8 overexpression promotes the degradation of VSV-G, leading to reduced expression in cells and incorporation into virions.

Similar experiments to those described above were performed with HIV-1 Env. MARCH8 expression significantly reduced the levels of both gp120 and gp41 in virions. The incorporation of WT gp120 was not impaired by expression of the MARCH8 mutants, while the MARCH8-W114A mutant modestly reduced (by ~40%) the levels of virion-associated gp120 for CTdel144 Env. The levels of virion-associated gp41 were markedly reduced for both WT and CTdel144 Env in the presence of MARCH8, and the MARCH8 mutants did not exert a statistically significant effect on virion gp41 levels (Fig. 4A and C). The reduced levels of virion-associated gp120 and gp41 imposed by MARCH8 expression are consistent with the infectivity data presented above (Fig. 2B). The expression of exogenous FLAG-tagged SGTA and HIV-1 Gag proteins in cells was similar across the different transfected samples, indicating that expression of WT and mutant MARCH8 is not cytotoxic under these conditions and no effect on virus particle production was observed (Fig. 4A). These results demonstrate that MARCH8 expression in the virus producer cell reduces the levels of virion-associated gp120 and gp41 for both WT and gp41 CT-deleted HIV-1 Env.

The EboV-GP bears a CT that contains only four residues, considerably shorter than the CT of either VSV-G or HIV-1 Env, yet it resembles HIV-1 Env in terms of the CT

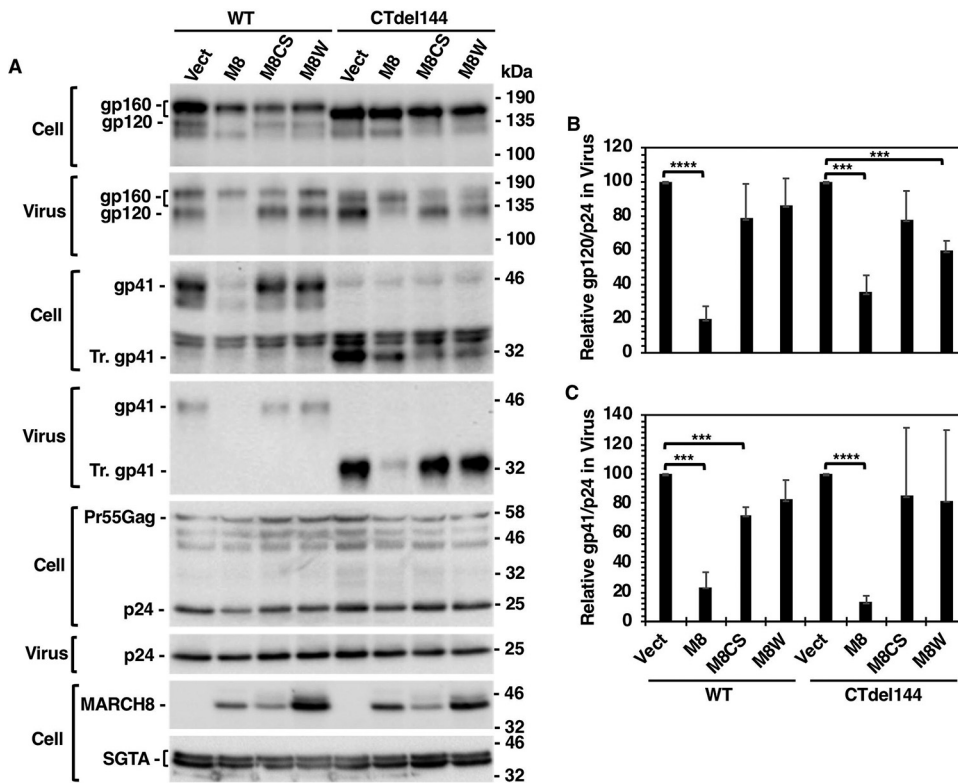


FIG 4 Effect of MARCH8 on HIV-1 Env processing and incorporation is CT independent. (A) HEK293T cells were cotransfected with pNL4-3 or pNL4-3/CTdel144 molecular clones (1 μ g) in the presence or absence of vectors expressing HA-tagged WT or mutant MARCH8 (100 ng) and FLAG-tagged SGTA as a transfection control. Two days posttransfection, cell and viral lysates were prepared and subjected to western blot analysis with anti-Env to detect gp160, gp120, and gp41, HIV-Ig to detect Gag proteins, Pr55Gag and p24 (CA), anti-HA to detect HA-tagged MARCH8, or anti-FLAG to detect FLAG-tagged SGTA. Mobility of molecular mass standards is shown on the right of the blots. Tr., truncated. (B) The levels of gp120 in virus was quantified and normalized to p24 and set at 100% in the absence of MARCH8. (C) The levels of gp41 in virus was quantified and normalized to p24, and set to 100% in the absence of MARCH8. Data shown are means plus SD from three independent experiments. Statistical significance (two-tailed unpaired *t* test): ***, $P < 0.001$; ****, $P < 0.0001$.

independence of its inhibition by MARCH8 in infectivity assays (Fig. 2). To investigate the effect of MARCH8 expression on the processing and incorporation of EboV-GP, we analyzed the levels of cell- and virion-associated EboV-GP in the presence and absence of MARCH8. The levels of cell- and virion-associated EboV-GP were significantly reduced in the presence of WT MARCH8, but not in the presence of the MARCH8-CS or MARCH8-W114A mutants (Fig. 5A and C). The incorporation of the Tailless and K-to-A EboV-GP mutants was also reduced in the presence of MARCH8 (Fig. 5A and B). We observed a significant reduction in the processing of EboV-GP0 in the presence of WT but not mutant MARCH8, as determined by the ratio of cell-associated GP0/GP1 (Fig. 5A and D). As observed with VSV-G and HIV-1 Env, overexpression of WT or mutant MARCH8 had no significant effect on cell-associated Gag expression or particle production (Fig. 5A). These observations demonstrate that the MARCH8-mediated infectivity defect observed with EboV-GP is due to impaired GP0 processing and correspondingly reduced virion incorporation of GP1 and GP2, and this defect is independent of the EboV-GP CT.

As mentioned in the introduction, MARCH8 expression has been reported to be high in the lung (51), making its effect on the respiratory virus SARS-CoV-2 of particular interest. Because the experiments described above demonstrated that neither inactive MARCH8 mutant (MARCH8-CS or MARCH8-W114A) was capable of consistent antiviral activity, in these and subsequent experiments, we used only one mutant, MARCH8-CS, as our negative control. As observed with HIV-1 Env and EboV-GP, the SARS-CoV-2 S

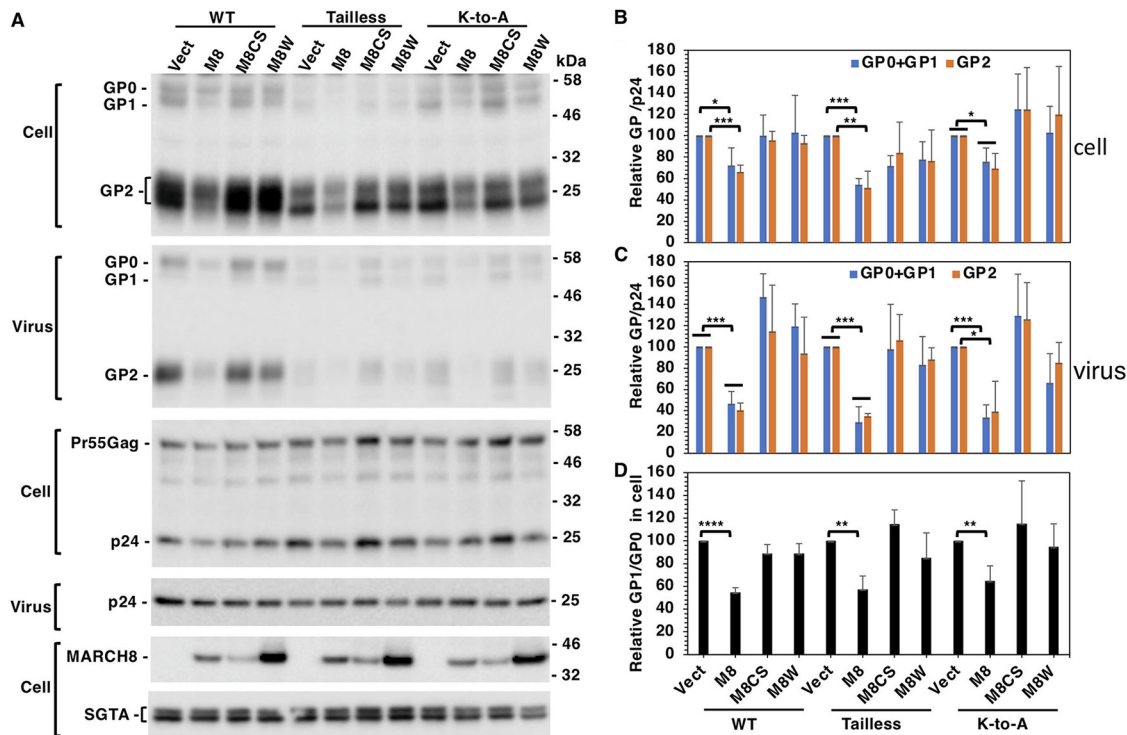


FIG 5 Effect of MARCH8 on processing and virion incorporation of EboV-GP is CT independent. (A) HEK293T cells were cotransfected with the Env-defective HIV-1 molecular clone pNL4-3/KFS (1 μ g) with vectors expressing WT or mutant EboV-GP (500 ng), HA-tagged WT or mutant MARCH8 (250 ng), and FLAG-tagged SGTA as a transfection control. Two days posttransfection, cell and viral lysates were prepared and subjected to western blot analysis with anti-EboV-GP Abs to detect pre-GP (G0), GP1, and GP2, HIV-Ig to detect Gag proteins, anti-HA to detect HA-tagged MARCH8, or anti-FLAG to detect FLAG-tagged SGTA. Mobility of molecular mass standards is shown on the right of the blots. (B) The levels of GP0 plus GP1 and GP2 in the cell were quantified, and the levels in the absence of MARCH8 were set at 100%. (C) The levels of GP0 plus GP1 and GP2 in virus were quantified, normalized to p24, and set at 100% in the absence of MARCH8. (D) The processing of EboV-GP in cells was quantified by calculating the ratio of GP1/GP0 and set at 100% for the no-MARCH8 control. Data shown are means plus SD from three independent experiments. Statistical significance (two-tailed unpaired *t* test): *, *P* < 0.05; **, *P* < 0.01; ***, *P* < 0.001; ****, *P* < 0.0001.

protein shows a CT-independent MARCH8-mediated restriction in infectivity assays (Fig. 2). To examine the effect of MARCH8 on SARS-CoV-2 S protein expression, we analyzed the levels of cell- and virion-associated S protein in the presence and absence of WT or catalytically inactive MARCH8. We observed that MARCH8 expression significantly reduced (by ~3- to 4-fold) the levels of S2 in cells and reduced S2 levels by ~10-fold in virions. Averaged over multiple assays, the MARCH8-CS mutant did not significantly reduce S protein levels (Fig. 6A and C). Consistent with the infectivity data presented above, the levels of the S protein mutants (K-to-R, CT-truncated, and CT-truncated K-to-R) were also reduced in the presence of MARCH8. We also observed a 60 to 70% reduction in the levels of WT and mutant S2 in the cell fraction in the presence of MARCH8, and we noted the presence of a smaller S2-related protein product (Fig. 6A, red arrow), which we speculate to be a less-glycosylated form of S2. The reductions in S2, and the presence of the smaller S2 species, were not observed upon expression of the MARCH8-CS mutant (Fig. 6A and B). The levels of the S precursor protein were not reduced by expression of MARCH8 in the virus producer cell, suggesting an effect primarily on S protein processing. These data demonstrate that expression of WT MARCH8 but not the MARCH8-CS mutant disrupts S protein processing, glycosylation, and incorporation into virus particles and indicate that the MARCH8-imposed antagonism of SARS-CoV-2 S protein is CT independent.

Because the effect of MARCH8 expression on both particle infectivity and glycoprotein levels in virions varied across the four viral glycoproteins studied here, we calculated the incorporation efficiency of each glycoprotein under the conditions used in

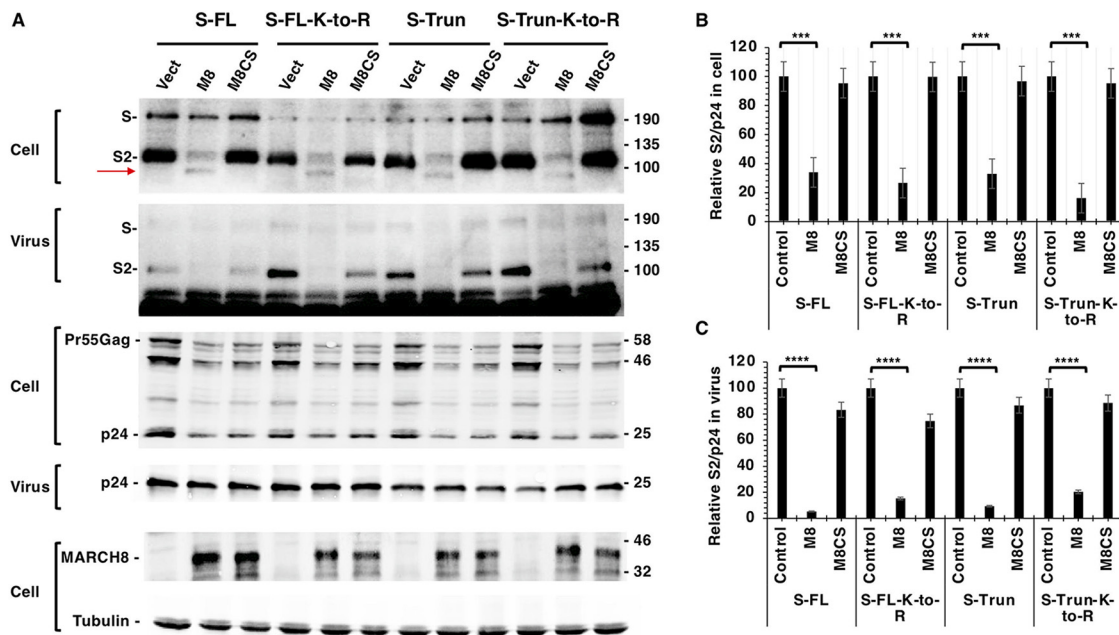


FIG 6 Effect of MARCH8 on processing and virion incorporation of SARS-CoV-2 S is CT independent. (A) HEK293T were cotransfected with the Env-defective, luciferase-expressing pNL4-3 derivative pNL4-3.Luc.R-E- ($3 \mu\text{g}$) with vectors expressing WT or mutant SARS-CoV-2 S protein (300 ng), and WT or mutant HA-tagged MARCH8 (200 ng). Two days posttransfection, cell and virus lysate were prepared and subjected to western blot analysis with anti-SARS-CoV-2 S2 Ab to detect precursor S and S2, HIV-Ig to detect Gag proteins, Pr55Gag and p24, and anti-HA to detect HA-tagged MARCH8. Molecular mass standards are shown on the right of the blots. The red arrow indicates a putative less-glycosylated form SARS-CoV-2 S2 protein in the cell lysate. (B) The level of SARS-CoV-2 S protein in cells was quantified and normalized to p24; values were set at 100% in the absence of MARCH8. (C) The level of S2 was quantified and normalized to p24 in virus; values were set at 100% in the absence of MARCH8. Data shown are means plus SD from three independent experiments. Statistical significance (two-tailed unpaired *t* test): ***, $P < 0.001$; ****, $P < 0.0001$.

the experiments described above (see Fig. S2 in the supplemental material). We observed that the EboV-GP incorporation efficiency was quite high, with nearly 40% of expressed GP present in VLPs. In contrast, the incorporation of SARS-CoV-2 S protein was quite low, perhaps because HIV-1 particles assemble on the plasma membrane, which, as noted in the introduction, is not the normal site of SARS-CoV-2 assembly. Incorporation efficiencies of HIV-1 gp41 and VSV-G were $\sim 18\%$ and $\sim 8\%$, respectively, under these experimental conditions (Fig. S2).

Knockdown of endogenous MARCH8 expression in HEK293T cells increases HIV-1 infectivity. Although levels of basal MARCH8 expression are known to be relatively low in established cell lines (51), we examined whether knockdown of *MARCH8* gene expression in HEK293T cells would affect the infectivity of HIV-1 particles produced from the *MARCH8*-depleted cells. HEK293T cells were treated with siRNA targeting MARCH8 or with a nontargeting control. *MARCH8* expression was measured by reverse transcription-quantitative PCR (RT-qPCR). At the highest siRNA input, *MARCH8* gene expression was reduced by approximately fivefold (Fig. 7A). Under these conditions, we observed a modest but statistically significant increase in the infectivity of HIV-1 particles produced from the *MARCH8*-depleted cells (Fig. 7B). The infectivity of virus produced from cells treated with the nontargeting siRNA control was not affected. These results demonstrate that even low levels of endogenous MARCH8 expression can impair HIV-1 infectivity.

MARCH8 expression is highly and rapidly inducible in certain cell types by IFN stimulation. Previous findings demonstrated that MARCH8 is highly expressed in MDMs in the absence of IFN stimulation and that expression levels are not appreciably increased in either MDMs or human CD4^+ T cells by overnight stimulation with alpha interferon (IFN- α) (11). Because IFN is known to induce highly variable levels of gene expression in a time-, dose-, and cell type-dependent manner (52, 53) and many genes

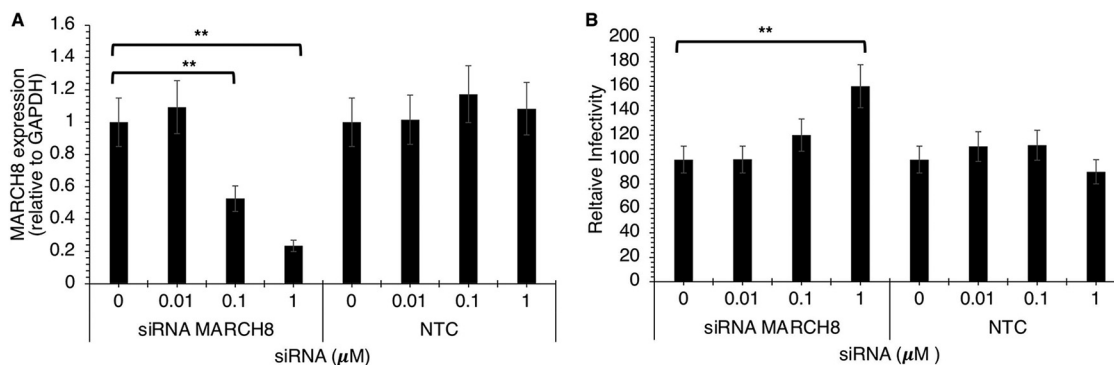


FIG 7 Knockdown of endogenous MARCH8 in HEK293T cells increases HIV-1 infectivity. (A) HEK293T cells were treated for 72 h with the indicated concentrations of MARCH8-specific siRNA or a nontargeting control (NTC). Endogenous *MARCH8* RNA expression was measured using RT-qPCR. GAPDH, glyceraldehyde-3-phosphate dehydrogenase. (B) siRNA-treated HEK293T cells in a 6-well plate were transfected with the pNL4-3 HIV-1 molecular clone (3 μg). Two days posttransfection, virus supernatants were collected, RT normalized, and used to infect TZM-bl cells. The infectivity in non-siRNA-treated cells is set at 100%. Data shown are means plus SD from three independent experiments. Statistical significance (two-tailed unpaired *t* test): **, *P* < 0.01.

with antiviral functions are IFN inducible (54), we performed RT-qPCR time course experiments with three different IFNs (IFN type I [α and β] and II [γ]) using total RNA extracted from different cell types and cell lines. We tested the SupT1 human T-cell line, primary hPBMCs from four different donors, the A549 transformed alveolar epithelial cell line, primary human airway epithelial cells, and HEK293T cells. In the SupT1 T-cell line, *MARCH8* gene expression was rapidly induced at 0.5 h poststimulation with IFN- α up to 70-fold over baseline levels, which subsided to ~10-fold over unstimulated levels by 4 h after induction (Fig. 8A) and then returned to baseline. Treatment with IFN- β induced an ~30-fold increase in *MARCH8* gene expression over baseline that peaked around 1 to 2 h post-IFN stimulation (Fig. 8A). To examine *MARCH8* gene expression in primary hPBMCs, cells from four donors were IFN stimulated and *MARCH8* RNA levels were measured. In three of the four donors, we observed that *MARCH8* expression increased five- to eightfold over unstimulated levels at 0.5 h poststimulation with IFN- α and then returned to baseline by 2 h poststimulation (Fig. 8B). In one donor, no IFN-inducible *MARCH8* gene expression was observed (data not shown). To investigate *MARCH8* gene expression in cells that are permissive for SARS-CoV-2 infection, we tested primary human airway epithelial cells and observed an ~3-fold increase in expression at 1 to 4 h after IFN- α stimulation (Fig. 8C). In HEK293T cells, we measured a rapid, ~7-fold increase in *MARCH8* gene expression after stimulation with IFN- α . Finally, we observed no IFN stimulation of *MARCH8* gene expression in A549 cells (data not shown). Collectively, these data indicate that *MARCH8* gene expression is induced to varying levels in cell lines and primary cell types that are natural targets for HIV-1 and SARS-CoV-2 infection.

It is important to verify that the levels of exogenous *MARCH8* gene expression achieved in these assays were not excessive relative to endogenous levels present in relevant cell types. Therefore, we investigated the *MARCH8* RNA expression levels in transiently transfected HEK293T cells upon increasing MARCH8 concentrations at 48 h posttransfection. The results indicated that *MARCH8* expression at 0.05 and 0.1 μg DNA input, the conditions used for the analyses presented in Fig. 2 to 6 was ~4- to 5-fold above the levels in untransfected cells (Fig. 8E). Transfection efficiencies were ~50% under these conditions (data not shown), indicating that transfected cells expressed *MARCH8* RNA at levels that were ~8- to 10-fold over those of untransfected cells. These results show that exogenous levels of *MARCH8* gene expression in our transfected 293T cells were lower than those observed following IFN stimulation of the SupT1 T-cell line and comparable to those measured in some IFN-stimulated hPBMC donors and HEK293T cells at early time points after IFN stimulation (Fig. 8A to D). The levels of basal expression of *MARCH8* relative to the housekeeping gene *GAPDH* in all of these cell types were comparable (see Table S1 in the

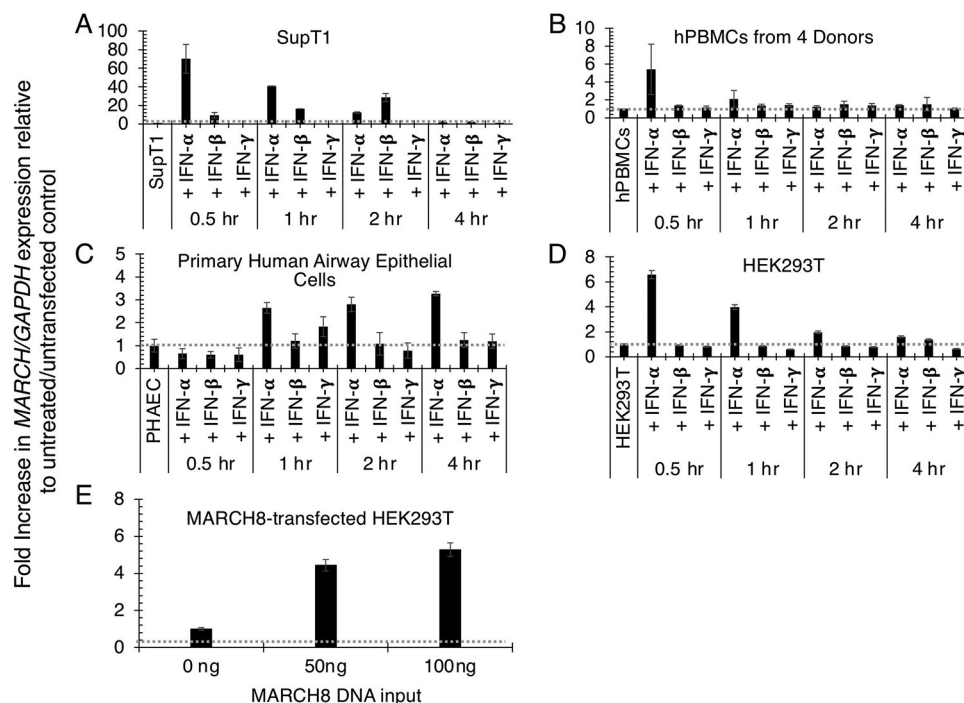


FIG 8 Endogenous *MARCH8* gene expression is rapidly induced by IFN. Endogenous *MARCH8* RNA expression in the SupT1 T-cell line (A), hPBMCs from 4 donors (B), primary human airway epithelial cells (C), and the HEK293T cell line (D) at 0, 0.5, 1, 2, and 4 h poststimulation with 1,000 U/ml type I (α and β) and II (γ) IFN. (E) *MARCH8* expression in transfected HEK293T cells 48 h posttransfection (hpt) with increasing concentrations of *MARCH8* expression vector (0, 50, and 100 ng) in a 6-well tissue culture plate. Isolated RNA was subjected to the RT-qPCR protocol as detailed in Materials and Methods. Fold increase in *MARCH8* RNA expression relative to untreated (A to D) or untransfected (E) controls is indicated. *MARCH8* RNA levels are expressed as a ratio of *MARCH8*/*GAPDH*. Data shown are means plus SD from three independent experiments.

supplemental material). Collectively, our data demonstrate that *MARCH8* gene expression can be induced rapidly by IFN stimulation in different cell types: a human T-cell line, hPBMCs, human airway epithelial cells, and the HEK293T cell line. The levels of exogenous expression in our transfected HEK293T cells were lower than, or comparable to, those achieved upon IFN stimulation at early time points in the T-cell line, primary hPBMCs, and HEK293T cells.

***MARCH8* retains VSV-G, HIV-1 Env, EboV-GP, and SARS-CoV-2 S protein in an intracellular compartment.** The western blotting data presented above demonstrate that *MARCH8* overexpression disrupts the processing and incorporation of viral envelope glycoproteins, suggesting that *MARCH8* might alter the trafficking of these viral glycoproteins. To examine the effect of *MARCH8* overexpression on the localization of different viral glycoproteins, we performed confocal microscopy using HEK293T cells transfected with *MARCH8* or the inactive *MARCH8*-CS mutant. Our confocal data showed that *MARCH8* localizes to the Golgi, a LAMP-1-positive (LAMP-1⁺) compartment, and the plasma membrane (Fig. S1) as previously reported (51). All of the viral glycoproteins and mutants used in this study colocalized with *MARCH8* and *MARCH8*-CS with strong Pearson's correlation coefficients (r) of ~ 0.7 to 0.9 (Table 1), indicating that *MARCH8* proteins and viral glycoproteins traffic through the same pathway. We quantified the intracellular colocalization between the dsRed-Golgi marker and the different viral glycoproteins in the presence of WT *MARCH8* and the inactive *MARCH8*-CS and observed strong colocalization ($r = \sim 0.7$ to 0.9) (Table 1 and Fig. 9 to 12).

In the absence of *MARCH8* overexpression, we observed WT VSV-G localization primarily in the Golgi and at the plasma membrane (Fig. 9A). *MARCH8* but not *MARCH8*-CS expression resulted in a marked shift in the localization of WT VSV-G from the plasma membrane to an intracellular vesicular compartment (Fig. 9A). The

TABLE 1 Colocalization of WT and mutant MARCH8, viral glycoproteins, and cellular markers

Viral GP ^a	<i>r</i> value ^b					
			+ MARCH8		+ MARCH8-CS	
	MARCH8	MARCH8-CS	Golgi-transferase ^c	LAMP-1	Golgi-transferase	LAMP-1
VSV-G	0.92 ± 0.08	0.82 ± 0.13	0.91 ± 0.03	0.89 ± 0.06	0.88 ± 0.01	0.16 ± 0.01
VSV-G Tailless	0.85 ± 0.11	0.80 ± 0.09	0.74 ± 0.14	0.31 ± 0.01	0.79 ± 0.15	0.18 ± 0.15
VSV-G K-to-R	0.83 ± 0.01	0.79 ± 0.01	0.90 ± 0.02	0.32 ± 0.04	0.85 ± 0.04	0.14 ± 0.04
HIV-1 Env	0.89 ± 0.13	0.79 ± 0.05	0.86 ± 0.07	0.79 ± 0.04	0.78 ± 0.02	0.18 ± 0.12
HIV-1 EnvCTdel144	0.87 ± 0.12	0.79 ± 0.02	0.79 ± 0.16	0.76 ± 0.04	0.79 ± 0.11	0.19 ± 0.02
EboV-GP	0.78 ± 0.06	0.73 ± 0.12	0.87 ± 0.11	0.67 ± 0.06	0.82 ± 0.08	0.12 ± 0.01
EboV-GP Tailless	0.82 ± 0.08	0.71 ± 0.15	0.81 ± 0.07	0.61 ± 0.21	0.79 ± 0.16	0.15 ± 0.13
SARS-CoV-2 S-FL	0.81 ± 0.01	0.72 ± 0.01	0.68 ± 0.13	0.65 ± 0.16	0.67 ± 0.08	0.20 ± 0.05
SARS-CoV-2 S-FL-K-to-R	0.86 ± 0.11	0.77 ± 0.05	0.67 ± 0.14	0.67 ± 0.21	0.69 ± 0.12	0.18 ± 0.06
SARS-CoV-2 S-Trun	0.89 ± 0.12	0.83 ± 0.03	0.79 ± 0.08	0.85 ± 0.08	0.78 ± 0.06	0.22 ± 0.14
SARS-CoV-2 S-Trun K-to-R	0.92 ± 0.06	0.86 ± 0.13	0.81 ± 0.1	0.81 ± 0.16	0.80 ± 0.21	0.14 ± 0.01

^aViral glycoprotein.

^bPearson correlation coefficient (*r*) values, means ± standard deviation (SD) using 50 cells per experimental condition. The *r* values indicate colocalization between MARCH8 and intracellular viral glycoprotein (first two columns), intracellular viral glycoprotein and cellular markers in the presence of WT MARCH8 (two middle columns), and intracellular viral glycoprotein and cellular markers in the presence of MARCH8-CS (right two columns).

^cGolgi-transferase = beta-1,4-galactosyltransferase.

predominantly plasma membrane localization of the VSV-G Tailless (Fig. 9B) and VSV-G K-to-R (Fig. 9C) mutants was not shifted by MARCH8 expression, consistent with the lack of MARCH8 targeting of these VSV-G mutants in infectivity and western blotting analyses. We observed a strong colocalization ($r \sim 0.89$) between WT VSV-G and the lysosomal marker LAMP-1 in the presence of WT MARCH8 expression (Fig. 9D; Table 1), whereas the Tailless and K-to-R VSV-G mutants showed low levels of colocalization with LAMP-1 ($r \sim 0.3$). In the presence of the inactive MARCH8-CS mutant, neither WT nor mutant VSV-G showed a high level of colocalization with LAMP-1 ($r \sim 0.2$) (Fig. 9E; Table 1). These data demonstrate that MARCH8 interferes with VSV-G trafficking and targets it to a LAMP-1-positive compartment in a manner that requires the Lys residues in the VSV-G CT.

We performed similar analyses with HIV-1 Env. As expected, WT and CTdel144 HIV-1 Env were observed in the Golgi and at the plasma membrane in the absence of MARCH8 expression (Fig. 10A and B). Similar to VSV-G, localization of WT HIV-1 Env was shifted in cells expressing MARCH8, and a high level of colocalization ($r \sim 0.8$) with LAMP-1 was observed (Fig. 10C and Table 1). In contrast to VSV-G, for which MARCH8-induced localization required the CT, the Tailless form of HIV-1 Env, CTdel144, was strongly localized to a LAMP-1⁺ compartment in MARCH8-expressing cells (Fig. 10C and Table 1). The inactive MARCH8-CS did not result in the retention of either WT or CTdel144 HIV-1 Env in a LAMP-1⁺ compartment (Fig. 10D). These findings are consistent with the infectivity and western blotting data presented above and indicate that the reductions in HIV-1 Env processing and incorporation in the presence of MARCH8 are associated with the retention of Env in an internal, LAMP-1⁺ compartment.

The confocal microscopy data obtained with EboV-GP and SARS-CoV-2 S protein paralleled our observations with HIV-1 Env but diverged from the results obtained with VSV-G. Expression of MARCH8 but not MARCH8-CS reduced the expression of these viral glycoproteins on the cell surface and induced their retention in an internal, LAMP-1⁺ compartment. The localization of truncated and K-to-R EboV-GP and S protein mutants was also shifted by MARCH8 expression (Fig. 11 and 12 and Table 1).

Taken together, the confocal microscopy data demonstrate that MARCH8 expression redirects the localization of viral glycoproteins by two distinct mechanisms. In the case of VSV-G, the CT is required for the MARCH8-induced relocation to a LAMP-1⁺ compartment, and mutation of the Lys residues in the CT abrogates the ability of MARCH8 expression to disrupt the localization of the viral glycoprotein. In contrast, for HIV-1 Env, EboV-GP, and SARS-CoV-2 S protein, neither the CT nor the Lys residues in the CT are required

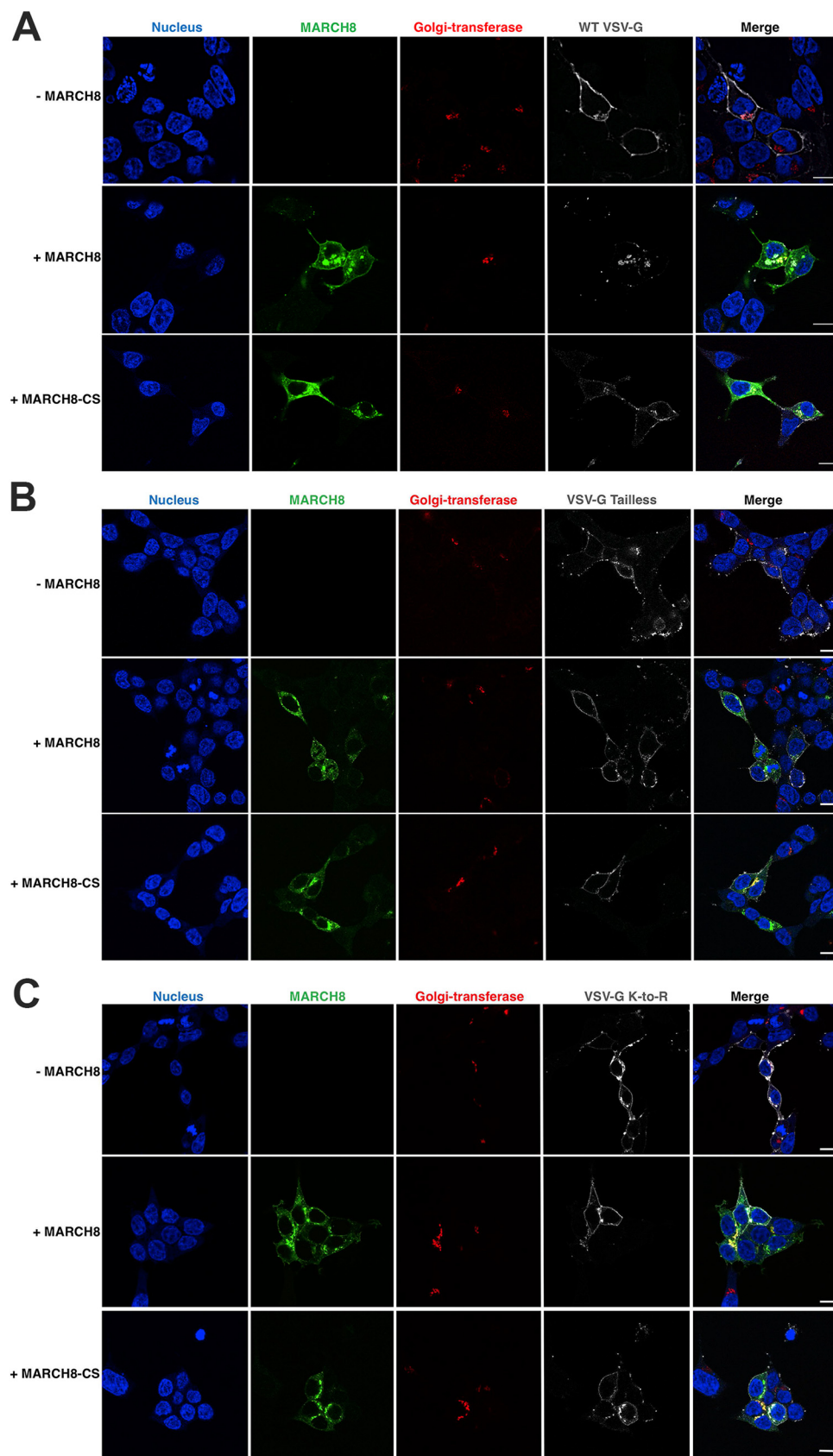


FIG 9 (Continued)

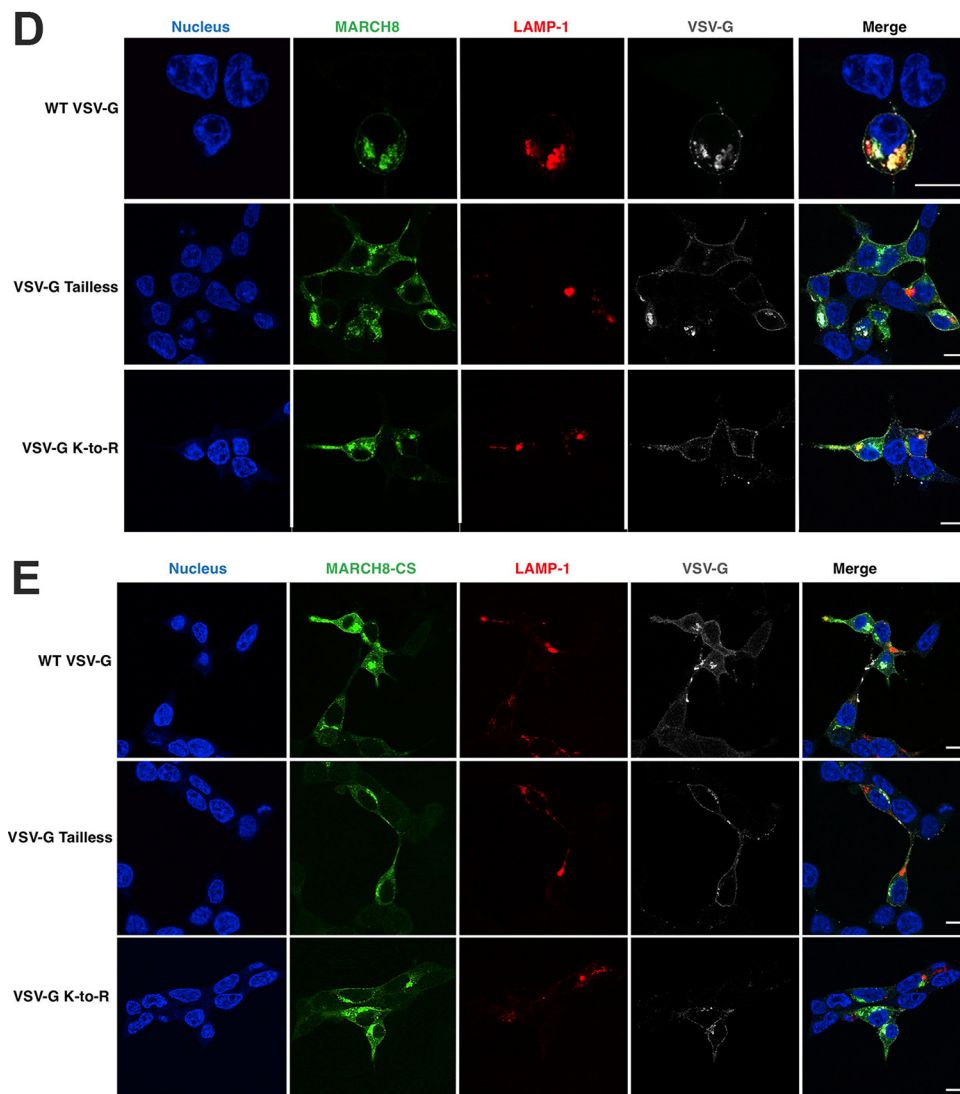


FIG 9 MARCH8 traps WT VSV-G, but not the VSV-G CT mutants, in an intracellular LAMP-1⁺ compartment. HEK293T cells were cotransfected with vectors expressing WT or mutant VSV-G (200 ng) with or without vectors expressing HA-tagged MARCH8, MARCH8-CS (100 ng), and the LAMP1-RFP or pDsRed-Golgi-Beta-1,4-galactosyltransferase (Golgi-transferase) (300 ng) expression vectors. One day posttransfection, cells were processed for confocal microscopy. (A to C) Distribution of WT VSV-G (A), VSV-G Tailless (B), or VSV-G K-to-R (C) in the absence (-) or presence (+) of WT MARCH8 or MARCH8-CS. (D and E) Colocalization of VSV-G or VSV-G mutants with WT MARCH8 (D) or MARCH8-CS (E) with the LAMP1-RFP or pDsRed-Golgi-Beta 1,4-galactosyltransferase cellular markers. Bars = 10 μ m.

for MARCH8-induced relocalization. The microscopy data are thus consistent with the infectivity and western blotting data (Fig. 2 and Fig. 3 to 6), showing that the ability of MARCH8 to antagonize VSV-G is dependent on the CT, but the antagonism of the other viral glycoproteins tested is CT independent.

DISCUSSION

In this study, we examined the ability of MARCH8 to antagonize a wide range of viral envelope glycoproteins—specifically, HIV-1 Env, VSV-G, EboV-GP, and SARS-CoV-2 S protein. Expression of MARCH8 in the virus producer cell reduced levels of viral glycoprotein processing for those glycoproteins that undergo furin-mediated cleavage, reduced glycoprotein stability, and interfered with glycoprotein incorporation into HIV-1 particles. In the case of VSV-G, MARCH8-mediated antagonism required the CT of the viral glycoprotein, and Lys residues in the CT were essential for MARCH8 restriction.

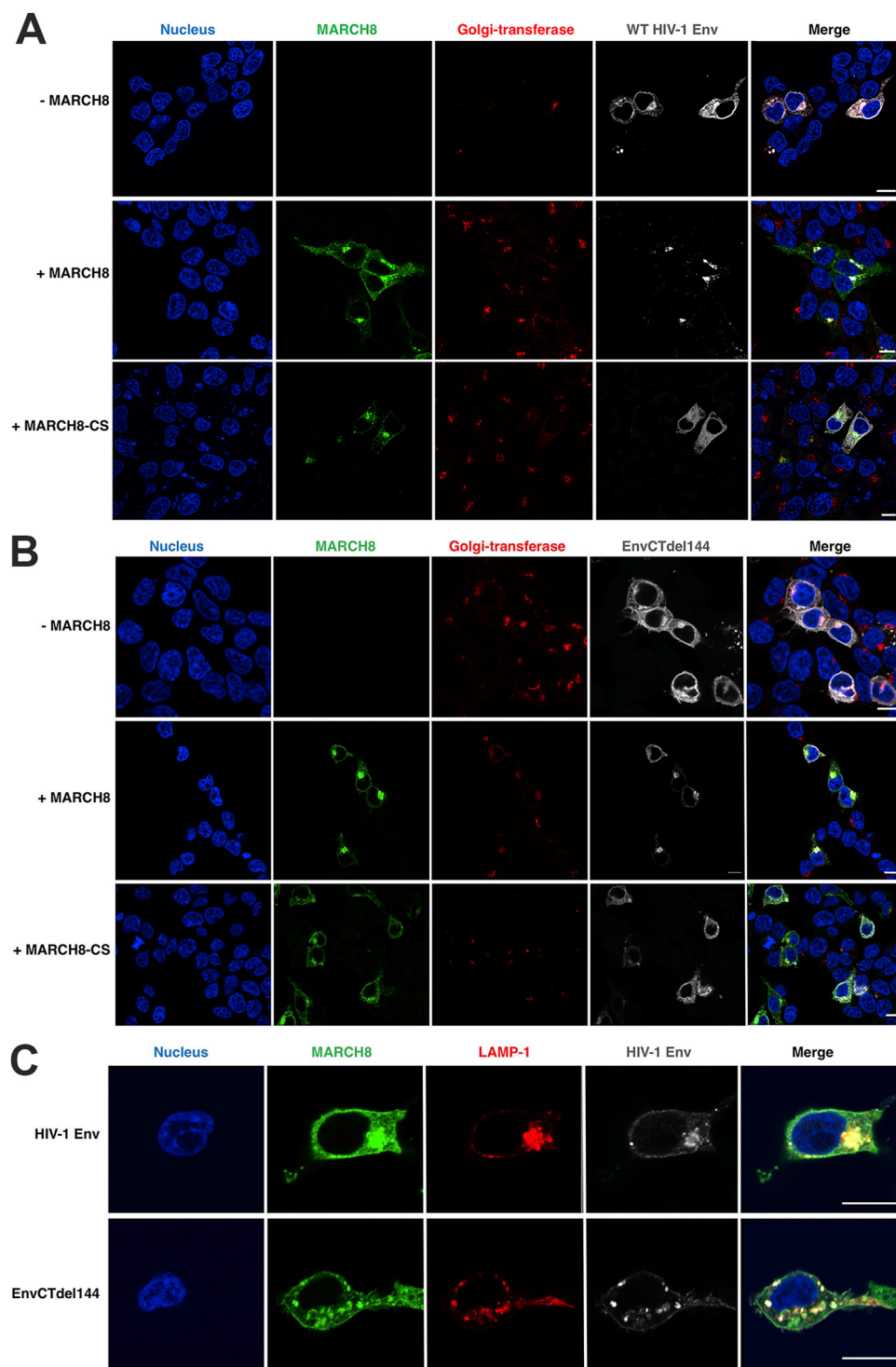


FIG 10 MARCH8 traps WT and truncated HIV-1 Env in an intracellular LAMP-1⁺ compartment. HEK293T cells were cotransfected with vectors expressing WT or truncated HIV-1 Env (pIIINL4-Env or pIIINL4-EnvCTdel144, respectively) (200 ng), pSV-Tat, and HA-tagged MARCH8 expression vectors (100 ng) and the LAMP1-RFP or pDsRed-Golgi-Beta 1,4-galactosyltransferase (300 ng) expression vectors. One day posttransfection, cells were processed for confocal microscopy. (A and B) Distribution of WT HIV-1 Env (A), and EnvCTdel144 (B) in the absence or presence of WT MARCH8 or MARCH8-CS. (C and D) Colocalization of HIV-1 Env and EnvCTdel144 with MARCH8 (C) and MARCH8-CS (D) and the LAMP1-RFP or pDsRed-Golgi-Beta 1,4-galactosyltransferase cellular markers. Bars = 10 μ m.

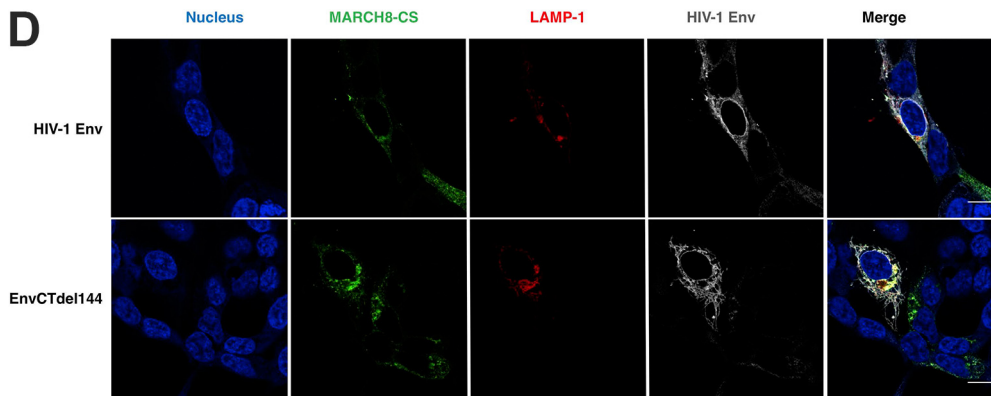


FIG 10 (Continued)

In contrast, in the case of HIV-1 Env, EboV-GP, and SARS-CoV-2 S protein, the CT of the viral glycoprotein was not required for the antiviral effect. In all cases, however, the ubiquitin ligase activity of MARCH8 was required for restriction, as RING domain mutations to a large extent abrogated the inhibition. While this article was being prepared, another group reported that, as we observed here, MARCH8-mediated restriction of VSV-G was CT dependent, but antagonism of HIV-1 Env was CT independent, and they demonstrated MARCH8-mediated ubiquitination of VSV-G (55). These results support a model whereby the RING domain E3 ubiquitin ligase activity of MARCH8 either directly targets the CT of the viral glycoprotein—as has been shown for MARCH protein-mediated downregulation of a variety of cellular proteins (18)—or exerts its effect indirectly. In either case, the consequence of MARCH8 activity is the apparent redirection of the viral glycoproteins to a LAMP-1⁺ compartment. This is consistent with MARCH8 inducing lysosomal degradation of viral glycoproteins.

While MARCH8 expression antagonized each of the glycoproteins tested here, the magnitude of the effect varied across the different glycoproteins, in terms of both particle infectivity and glycoprotein incorporation into virions. Specifically, the inhibition of VSV-G and HIV-1 Env was quite severe, whereas more modest effects were observed with EboV-GP and SARS-CoV-2 S. The degree of inhibition did not correlate with the viral glycoprotein incorporation efficiency; for example, EboV-GP was very efficiently incorporated into HIV-1 particles, whereas SARS-CoV-2 S protein was inefficiently incorporated. Further study will be required to determine the basis for the variable activity of MARCH8 against the four glycoproteins examined in this study.

It remains unclear at what stage during their trafficking pathway viral glycoproteins are targeted by MARCH8. MARCH8 could act early during trafficking of the viral glycoprotein through the Golgi *en route* to the site of virus assembly, at the plasma membrane, or, in the case of glycoproteins like HIV-1 Env that undergo a recycling step, could act late following endocytic uptake from the plasma membrane. MARCH proteins have been reported to target a large repertoire of cellular proteins, including innate/adaptive immune receptors and intracellular adhesion molecules (18). Previous studies have shown that the overexpression of MARCH proteins can cause redistribution of syntaxin 4 and syntaxin 6 as well as some syntaxin-6-interacting soluble *N*-ethylmaleimide-sensitive factor attachment protein receptors (SNAREs), which are known to be involved in cellular endosomal trafficking (56, 57). MARCH protein overexpression has also been reported to alter the trafficking of clathrin-independent endocytosis (CIE) cargo proteins, rerouting them to endosomes and lysosomes for degradation (29). Thus, the indirect mechanism of MARCH8-mediated targeting of viral glycoproteins that we hypothesize would involve the ubiquitination and downregulation of a cellular factor(s) involved in viral glycoprotein trafficking. The resulting accumulation

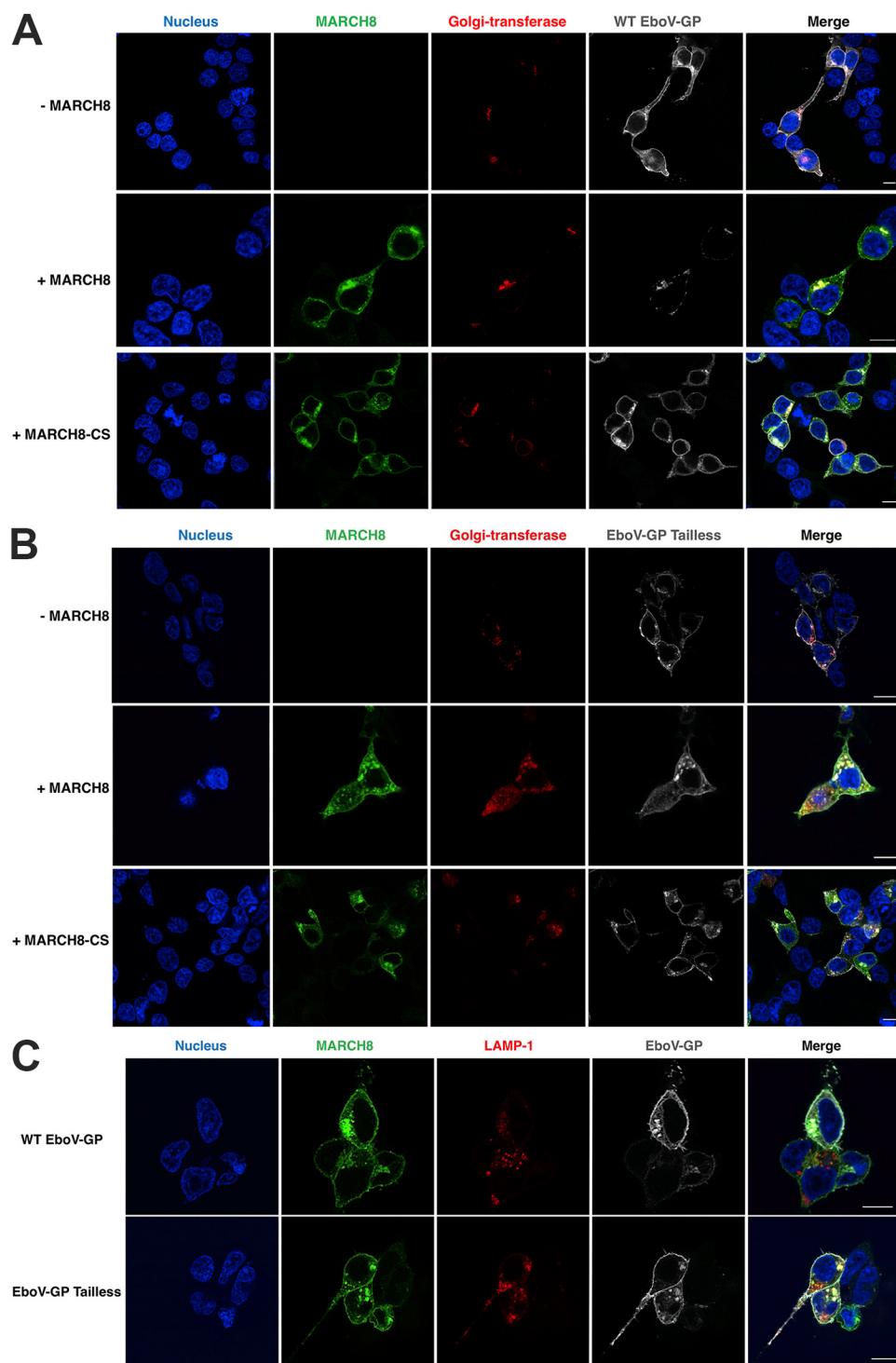


FIG 11 MARCH8 traps WT and truncated EboV-GP in an intracellular LAMP-1⁺ compartment. HEK293T cells were cotransfected with vectors expressing EboV-GP or EboV-GP Tailless (200 ng) and HA-tagged MARCH8 expression vectors (100 ng) and the LAMP1-RFP or pDsRed-Golgi-Beta 1,4-galactosyltransferase (300 ng) expression vectors. One day posttransfection, cells were processed for confocal microscopy. (A and B) Distribution of EboV-GP (A) and EboV-GP Tailless (B) in the absence or presence of WT MARCH8 or MARCH8-CS. (C and D) Colocalization of EboV-GP and EboV-GP Tailless with MARCH8 (C) and MARCH8-CS (D) and the LAMP1-RFP or pDsRed-Golgi-Beta 1,4-galactosyltransferase cellular markers. Bars = 10 μ m.

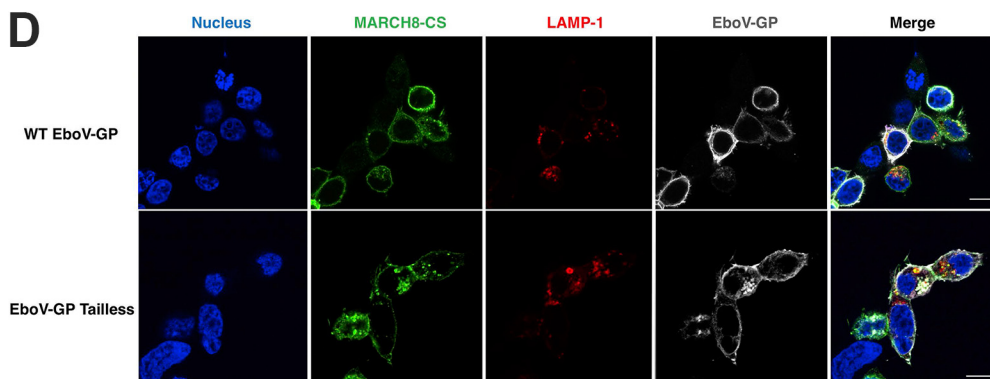


FIG 11 (Continued)

of the viral glycoprotein in a LAMP-1⁺ intracellular compartment (Fig. 9 to 12) would reduce virion incorporation of the viral glycoprotein and impair particle infectivity. Taken together, our data suggest that MARCH8 exerts its antiviral activity via two different mechanisms, one (e.g., as observed for VSV-G) in which the CT of the viral glycoprotein is directly ubiquitinated, the other (e.g., as observed for HIV-1 Env, EboV-GP, and SARS-CoV-2 S) in which a host trafficking factor(s) is targeted, resulting in an indirect restriction of the viral glycoprotein.

The viral homologs of the cellular MARCH proteins have been reported to ubiquitinate residues other than Lys in the CTs of their target proteins; for example, the K3 protein of KSHV has been reported to attach ubiquitin to Cys residues, and the mk3 protein of gamma herpesviruses can ubiquitinate Ser and Thr in addition to Lys (35–37, 58). It is not clear whether MARCH proteins are able to ubiquitinate non-Lys residues, but we cannot exclude this possibility. Inspection of the viral glycoproteins under study indicates that the truncated HIV-1 Env mutant CTdel144 and EboV-GP Tailless have no Ser, Thr, or Cys residues facing the cytosol, indicating that their CTs cannot be ubiquitinated. In contrast, SARS-CoV-2 S-Trun has 4 Ser, 1 Thr, and 10 Cys residues. Ongoing work is investigating whether the CT of SARS-CoV-2 S protein undergoes MARCH8-mediated ubiquitination. It is interesting to note that the basic residues in the CT of HIV-1 gp41 are highly skewed toward Arg instead of Lys residues; for example, the CT of the NL4-3 strain of HIV-1 used in this study contains 21 Arg residues but only two Lys residues (<https://www.hiv.lanl.gov/content/sequence/HIV/mainpage.html>). This observation invites the speculation that HIV-1 may have evolved to limit the number of Lys residues available for gp41 CT ubiquitination.

Our results show a broad antiviral activity of MARCH8 against the glycoproteins from three human viral pathogens—HIV-1, EboV, and SARS-CoV-2—and a primarily animal pathogen, VSV. MARCH8 targeting of HIV-1 Env, VSV-G, and, very recently, EboV-GP, has been reported (6, 8, 11, 55, 59). HIV-1 replicates predominantly in CD4⁺ T cells and also infects MDMs (60). EboV targets mainly alveolar macrophages and endothelial cells (61). SARS-CoV-2, like other coronaviruses, targets airway epithelial cells (62). VSV typically replicates in cells of the oral mucosa, although VSV-G confers very broad tissue tropism (63). In this study, we relied extensively on expressing MARCH8 exogenously to evaluate its effect on viral envelope glycoprotein stability, trafficking, and incorporation. This raises the question of whether the levels of MARCH8 expression achieved in these experiments are physiologically relevant. A previous study demonstrated that depletion of MARCH8 in primary human MDMs significantly increased the infectivity of HIV-1 particles released from these cells, suggesting that at least in this cell type endogenous levels of MARCH8 expression are sufficient to restrict HIV-1 infectivity (11). MARCH8 expression is high in the lung (19), suggesting its potential relevance to infection by respiratory viruses like SARS-CoV-2. Due to the poor quality

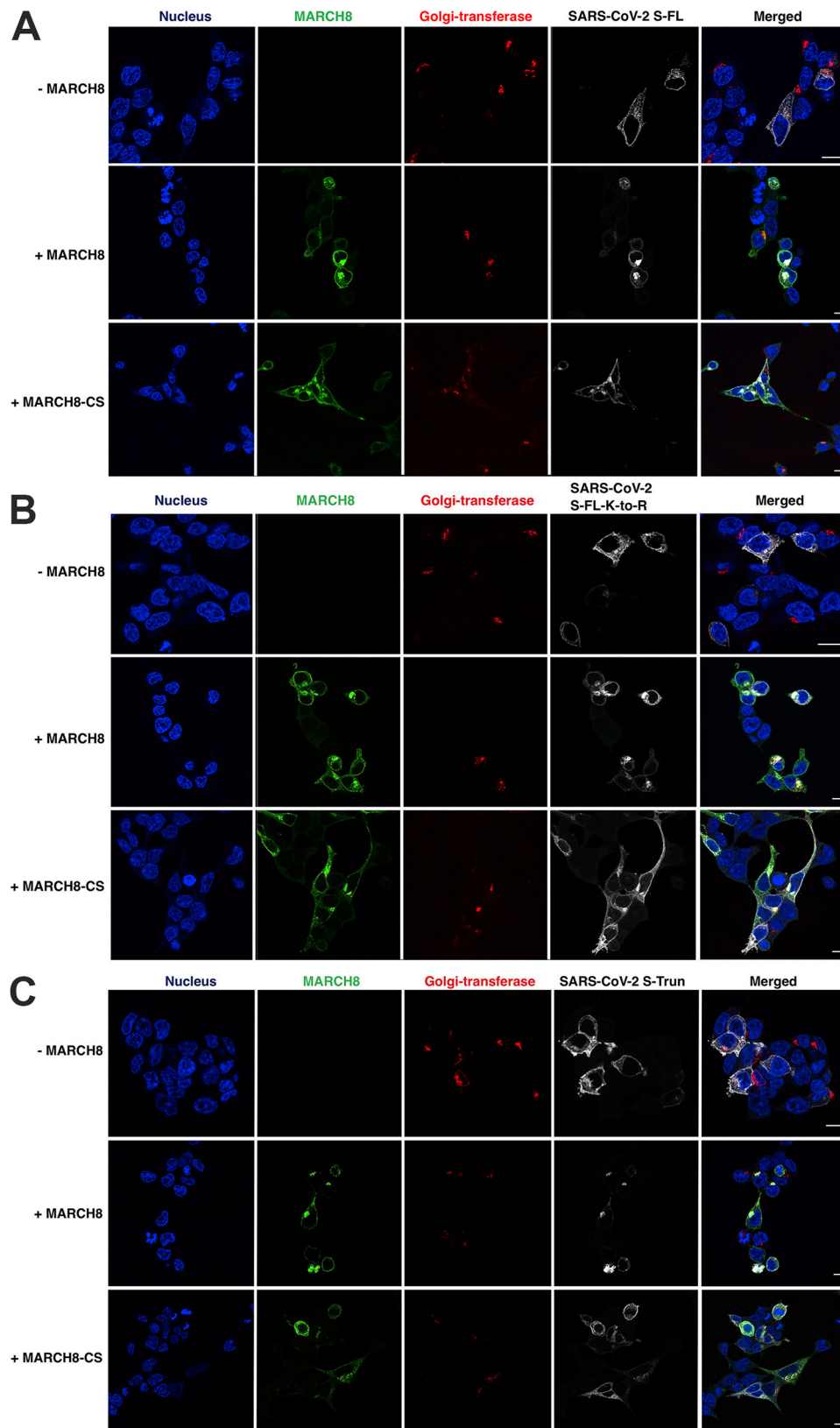


FIG 12 (Continued)

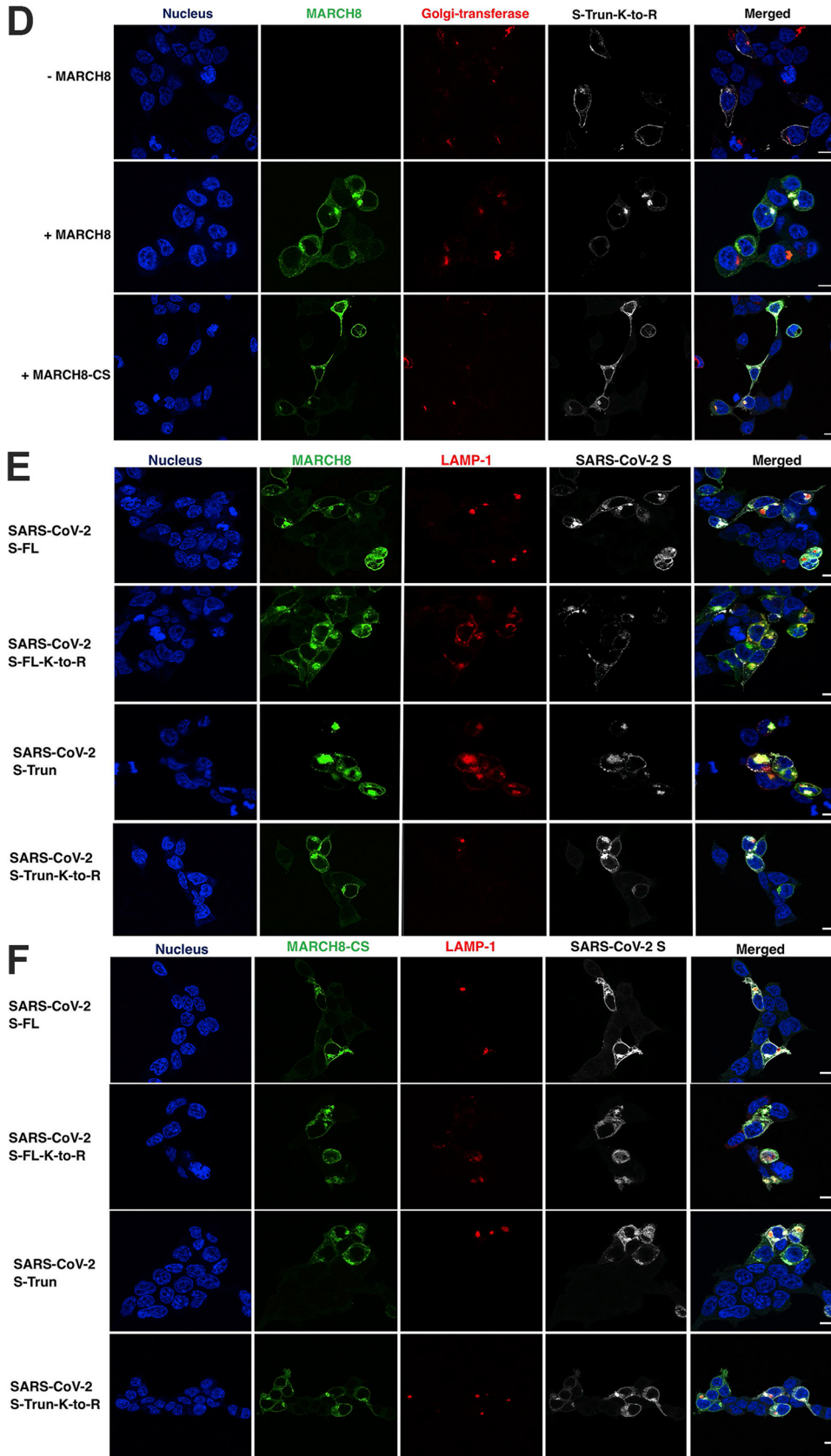


FIG 12 (Continued)

of available MARCH8 antibodies, we could not evaluate endogenous MARCH8 protein expression. Instead, RT-qPCR was used to measure the endogenous *MARCH8* gene expression in relevant cell types in the presence and absence of IFN. In the absence of IFN stimulation, basal levels of *MARCH8* RNA, measured as a ratio to *GAPDH*, were similar across the cell types analyzed. The RNA levels measured following IFN induction were comparable to those in transiently transfected HEK293T cells. Although RNA levels may not be directly correlated with protein expression, the results suggest that the MARCH8 expression in the cell types tested may be sufficient to exert an antiviral activity. Indeed, even in the absence of IFN stimulation, we observed that depletion of MARCH8 in HEK293T cells caused a modest but statistically significant increase in the infectivity of particles produced from those cells. In addition, our data indicate that *MARCH8* is an IFN-stimulated gene (ISG). The type I IFN (IFN-I) response is crucial in the host antiviral defense against viral infections (64, 65). A recent publication highlighted the importance of the IFN-I response in immune protection against SARS-CoV-2 by establishing a link between life-threatening coronavirus disease 2019 (COVID-19) symptoms and loss-of-function mutations in IFN-I-related genes (66).

Viruses, including those whose envelope glycoproteins were studied here, have evolved a complex array of countermeasures to disable the function of cellular ISGs (67). Further work will be required to elucidate mechanisms by which viruses counteract the antiviral activity of the MARCH family of E3 ubiquitin ligases.

MATERIALS AND METHODS

Cell culture. HEK293T cells (obtained from the American Type Culture Collection [ATCC]) and TZM-bl cells (obtained from J. C. Kappes, X. Wu, and Tranzyme, Inc. through the NIH AIDS Reagent Program [ARP], Germantown, MD) were maintained in Dulbecco modified Eagle medium (DMEM) containing 5% or 10% (vol/vol) fetal bovine serum (FBS; HyClone), 2 mM glutamine, 1% penicillin-streptomycin (penicillin [50 U/ml] and streptomycin [50 µg/ml] [final concentration]; Lonza) at 37°C with 5% CO₂. The SupT1 T-cell line was cultured in RPMI with 10% FBS and 1% penicillin-streptomycin. The A549 human lung epithelial cell line (obtained from the ATCC) was cultured in DMEM with 10% FBS and 1% penicillin-streptomycin. Primary small airway epithelial cells (obtained from ATCC) were cultured in airway epithelial cell basal medium (ATCC) supplemented with bronchial epithelial cell growth kit (ATCC). Primary hPBMCs were obtained from healthy volunteers from the National Cancer Institute (NCI)-Frederick Research Donor Program. The hPBMCs were extracted from whole blood using the Histopaque procedure (Sigma). Cells were then stimulated with phytohemagglutinin P (PHA-P) and IL-2 for 3 days.

Plasmids and transfection. The following plasmids were used in this study: the full-length HIV-1 clade B molecular clone pNL4-3 and derivatives pNL4-3EnvCTdel144 (68), pNL4-3KFS (*env*-minus) (69), pNL4-3.Luc.R-E- (NIH ARP, catalog number 3418); and the pHCMV-G (VSV-G expression vector) (70, 71). The EboV-GP ΔMLD was a gift from Judith White (University of Virginia) (47), and SARS-CoV-2 S protein (full-length [FL] and truncated) expression vectors were gifts from Thomas Gallagher (Loyola University). The MARCH8 and MARCH8-CS plasmids were gifts from Kenzo Tokunaga (National Institute of Infectious Diseases, Tokyo, Japan). Viral glycoprotein mutant plasmids VSV-G Tailless, VSV-G K-to-A, and VSV-G K-to-R, EboV-GP K-to-A and EboV-GP-Tailless, SARS-CoV-2 S-FL K-to-R, and SARS-CoV-2 S-Truncated K-to-R were generated using the Q5 site-directed mutagenesis kit (New England BioLabs Inc., catalog number E05525) or the QuikChange site-directed mutagenesis kit (Stratagene) according to the manufacturer's instructions with primers listed in Table S2 in the supplemental material. In microscopy experiments, pDsRed-monomer-Golgi-Beta-1,4-galactosyltransferase (Clontech, catalog number 632480) and LAMP-RFP (red fluorescent protein) (Addgene, catalog number 1817) (72) were used. Plasmids were purified using MaxiPrep kits (Qiagen, catalog number 12263), and mutations were verified by sequencing (Psomagen, Rockville, MD). The HEK293T cells were transfected with the indicated plasmids using polyethyleneimine (PEI) or Lipofectamine 2000 (Invitrogen) according to the manufacturer's instructions. Virus-containing supernatants were filtered through 0.45-µm membrane 24 or 48 h posttransfection, and virus was quantified by measuring reverse transcriptase (RT) activity. Virus-containing supernatant was harvested 24 or 48 h posttransfection, and virus particles were collected by ultracentrifugation.

FIG 12 MARCH8 traps WT and CT-mutant SARS-CoV-2 S proteins in an intracellular LAMP-1⁺ compartment. HEK293T cells were cotransfected with vectors expressing WT or CT-mutant SARS-CoV-2 S proteins (200 ng) and HA-tagged MARCH8 expression vectors (100 ng) and the LAMP1-RFP or pDsRed-Golgi-Beta 1,4-galactosyltransferase (300 ng) expression vectors. One day posttransfection, cells were processed for confocal microscopy. (A to D) Distribution of SARS-CoV-2 S-FL (A), SARS-CoV-2 S-FL-K-to-R (B), SARS-CoV-2 S-Trun (C) and SARS-CoV-2 S-Trun-K-to-R (D) in the presence of MARCH8 and MARCH8-CS. (E and F) Colocalization of SARS-CoV-2 S WT and CT mutants with MARCH8 (E) and MARCH8-CS (F) and the LAMP1-RFP or pDsRed-Golgi-Beta 1,4-galactosyltransferase cellular markers. Bars = 10 µm.

Virus and cell pellets were solubilized in lysis buffer (10 mM iodoacetamide [Sigma-Aldrich], Complete protease inhibitor tablets [Roche], 300 mM sodium chloride, 50 mM Tris-HCl [pH 7.5], and 0.5% Triton X-100 [Sigma-Aldrich]) and used for further analysis.

Western blotting. Cell and virus lysates in lysis buffer with 6× sodium dodecyl sulfate-polyacrylamide gel electrophoresis (SDS-PAGE) sample loading buffer (600 mM Tris-HCl [pH 6.8], 30% glycerol, 12% SDS, 20 mM dithiothreitol [DTT], 0.03% bromophenol blue) were heated at 95°C for 5 min. Samples were analyzed on 10% 1.5-mm Tris-glycine gels using a Bio-Rad Trans-Blot Turbo Transfer system according to the manufacturer's instructions. Proteins were detected with primary antibodies (see Table S3) and secondary antibodies. Protein bands were visualized using chemiluminescence with either a Gel Doc XR+ system (Bio-Rad) or Sapphire biomolecular imager (Azure Biosystems) and analyzed with either Image Lab version 6.0.1 or AzureSpot (Azure Biosystems).

Single-cycle infectivity assays. TZM-bl is a HeLa-derived cell line that contains a stably integrated HIV-LTR-luciferase construct (LTR stands for long terminal repeat) (73, 74). TZM-bl cells were infected with serial dilutions of RT-normalized virus stock (44) in the presence of 10 μg/ml DEAE-dextran. For SARS-CoV-2 S infectivity assays, HEK293T cells stably expressing hACE2 (BEI Resources, catalog number NR-52511) were infected with serial dilutions of RT-normalized S-pseudotyped, luciferase-expressing HIV-1 (pNL4-3.Luc.R-E-) virus stock in the presence of 10 μg/ml DEAE-dextran. Cells were lysed with BriteLite luciferase reagent (Perkin-Elmer), and luciferase was measured in a Wallac BetaMax plate reader at 48 h postinfection. Data were normalized to data for non-MARCH-transfected negative control from three independent experiments.

Confocal microscopy. Microscopy experiments used 18-mm coverslips (Electron Microscopy Sciences, catalog number 72291-06) which were sterilized by soaking in ethanol and air dried before seeding of HEK293T cells. Coverslips were pretreated with fibronectin (Sigma-Aldrich, catalog number GC010) at 1:50 dilution in phosphate-buffered saline (PBS) for 30 min at room temperature before seeding cells. HEK293T cells were cultured overnight, fixed with 4% paraformaldehyde (Electron Microscopy Sciences, catalog number BM-155) at 24 h posttransfection in Dulbecco PBS (DPBS) for 1 h, and quenched with 0.1 M glycine in PBS for 10 min. Cells were permeabilized with 0.2% Triton X-100 (Sigma-Aldrich, catalog number T-8787) in PBS for 5 min, blocked with PBS containing 10% bovine serum albumin (BSA) (Sigma-Aldrich) for 30 min and stained with primary antibodies at a 1:400 dilution with 0.1% Triton X-100 and 1% BSA in PBS for 1 h. After three washes in PBS, cells were incubated with secondary antibodies and 4',6'-diamidino-2-phenylindole (DAPI) stain in 1:1000 dilution in PBS. Antibody information is listed in Table S3. Cells were washed and mounted with Fluoromount-G (Electron Microscopy Sciences, catalog number 0100-01). Imaging was performed with a Leica TCS SP8 microscope (Leica Microsystems Inc., Buffalo Grove, IL) using a 63× oil-immersion objective. Images were generated using ImageJ software (NIH, Bethesda, MD). Background was subtracted using ImageJ's built-in "rolling ball" background subtraction process. Colocalization analyses were performed with an intracellular region of interest (ROI) excluding any plasma membrane-associated signal using colocalization test and a plugin, EzColocalization (75), with ImageJ. Untransfected cells were excluded from analysis.

RT-qPCR. To measure *MARCH8* expression levels, total RNA was extracted using RNeasy Plus minikit (Qiagen) following the manufacturer's instructions from transfected HEK293T cell lines or cells stimulated with 1,000 U/ml of IFN-α, -β, or -γ (PBL Assay Science, catalog number 11200, 11415, or 11500, respectively). RNA was transcribed using High-Capacity cDNA reverse transcription kit (Applied Biosystems), and real-time PCR was performed using KAPA Sybr Fast master mix (Kapa Biosystems) following the manufacturer's instructions using CFX connect real-time PCR detection system (Bio-Rad) with specific oligonucleotides described previously (6, 11). The *MARCH8* mRNA levels were normalized with *GAPDH* mRNA levels using the $\Delta\Delta C_T$ method for relative quantification.

siRNA knockdown of endogenous *MARCH8*. HEK293T cells were transfected with 0.01, 0.1, and 1 μM *MARCH8*-specific siRNA or nontargeting control (NTC) (Smart pool, Dharmacon) using Lipofectamine RNAiMAX (ThermoFisher Scientific) following the manufacturer's protocol. Seventy-two hours after siRNA treatment, cells were collected for RT-qPCR to measure *MARCH8* expression. The siRNA-treated HEK293T cells were transfected with the HIV-1 pNL4-3 clone, and the progeny viruses were collected at 48 h posttransfection, RT normalized, and used to infect the TZM-bl indicator cell line.

SUPPLEMENTAL MATERIAL

Supplemental material is available online only.

FIG S1, TIF file, 0.8 MB.

FIG S2, TIF file, 0.5 MB.

TABLE S1, TIF file, 0.9 MB.

TABLE S2, TIF file, 2.3 MB.

TABLE S3, TIF file, 1.6 MB.

ACKNOWLEDGMENTS

We thank Kenzo Tokunaga, Judith White, and Thomas Gallagher for providing plasmids for the study. We thank Sherimay Ablan and Melissa V. Fernandez for technical advice and members of the Freed lab for critical review of the manuscript and helpful discussion. We thank Kim Peifley and David Scheiblin (NCI-Frederick) for technical advice on microscopy.

Research in the Freed lab is supported by the Intramural Research Program of the Center for Cancer Research, National Cancer Institute, National Institutes of Health. Funds were also provided by a grant from the Intramural Targeted Anti-COVID-19 (ITAC) Program and from an Intramural AIDS Research Fellowship (for C.M.L.).

C.M.L., A.A.W., and E.O.F. designed research. C.M.L., A.A.W., A.M., and N.P. performed research. C.M.L. and A.A.W. analyzed data. C.M.L., A.A.W., and E.O.F. wrote the paper.

REFERENCES

- Ghimire D, Rai M, Gaur R. 2018. Novel host restriction factors implicated in HIV-1 replication. *J Gen Virol* 99:435–446. <https://doi.org/10.1099/jgv.0.001026>.
- Forlani G, Shallak M, Ramia E, Tedeschi A, Accolla RS. 2019. Restriction factors in human retrovirus infections and the unprecedented case of CIITA as link of intrinsic and adaptive immunity against HTLV-1. *Retrovirology* 16:34. <https://doi.org/10.1186/s12977-019-0498-6>.
- Jia X, Zhao Q, Xiong Y. 2015. HIV suppression by host restriction factors and viral immune evasion. *Curr Opin Struct Biol* 31:106–114. <https://doi.org/10.1016/j.sbi.2015.04.004>.
- D'Urbano V, De Crignis E, Re MC. 2018. Host restriction factors and human immunodeficiency virus (HIV-1): a dynamic interplay involving all phases of the viral life cycle. *Curr HIV Res* 16:184–207. <https://doi.org/10.2174/1570162X16666180817115830>.
- Beitari S, Wang Y, Liu SL, Liang C. 2019. HIV-1 envelope glycoprotein at the interface of host restriction and virus evasion. *Viruses* 11:311. <https://doi.org/10.3390/v11040311>.
- Zhang Y, Tada T, Ozono S, Yao W, Tanaka M, Yamaoka S, Kishigami S, Fujita H, Tokunaga K. 2019. Membrane-associated RING-CH (MARCH) 1 and 2 are MARCH family members that inhibit HIV-1 infection. *J Biol Chem* 294:3397–3405. <https://doi.org/10.1074/jbc.AC118.005907>.
- Braun E, Hotter D, Koepke L, Zech F, Groß R, Sparrer KMJ, Müller JA, Pfaller CK, Heusinger E, Wombacher R, Sutter K, Dittmer U, Winkler M, Simmons G, Jakobsen MR, Conzelmann K-K, Pöhlmann S, Münch J, Fackler OT, Kirchhoff F, Sauter D. 2019. Guanylate-binding proteins 2 and 5 exert broad antiviral activity by inhibiting furin-mediated processing of viral envelope proteins. *Cell Rep* 27:2092–2104.e10. <https://doi.org/10.1016/j.celrep.2019.04.063>.
- Zhang Y, Lu J, Liu X. 2018. MARCH2 is upregulated in HIV-1 infection and inhibits HIV-1 production through envelope protein translocation or degradation. *Virology* 518:293–300. <https://doi.org/10.1016/j.virol.2018.02.003>.
- Hotter D, Sauter D, Kirchhoff F. 2017. Guanylate binding protein 5: impairing virion infectivity by targeting retroviral envelope glycoproteins. *Small GTPases* 8:31–37. <https://doi.org/10.1080/21541248.2016.1189990>.
- Krapp C, Hotter D, Gawanbacht A, McLaren PJ, Kluge SF, Sturzel CM, Mack K, Reith E, Engelhart S, Ciuffi A, Hornung V, Sauter D, Telenti A, Kirchhoff F. 2016. Guanylate binding protein (GBP) 5 is an interferon-inducible inhibitor of HIV-1 infectivity. *Cell Host Microbe* 19:504–514. <https://doi.org/10.1016/j.chom.2016.02.019>.
- Tada T, Zhang Y, Koyama T, Tobiume M, Tsunetsugu-Yokota Y, Yamaoka S, Fujita H, Tokunaga K. 2015. MARCH8 inhibits HIV-1 infection by reducing virion incorporation of envelope glycoproteins. *Nat Med* 21:1502–1507. <https://doi.org/10.1038/nm.3956>.
- Sood C, Marin M, Chande A, Pizzato M, Melikyan GB. 2017. SERINC5 protein inhibits HIV-1 fusion pore formation by promoting functional inactivation of envelope glycoproteins. *J Biol Chem* 292:6014–6026. <https://doi.org/10.1074/jbc.M117.777714>.
- Usami Y, Wu Y, Gottlinger HG. 2015. SERINC3 and SERINC5 restrict HIV-1 infectivity and are counteracted by Nef. *Nature* 526:218–223. <https://doi.org/10.1038/nature15400>.
- Rey FA, Lok SM. 2018. Common features of enveloped viruses and implications for immunogen design for next-generation vaccines. *Cell* 172:1319–1334. <https://doi.org/10.1016/j.cell.2018.02.054>.
- Tang T, Bidon M, Jaimes JA, Whittaker GR, Daniel S. 2020. Coronavirus membrane fusion mechanism offers a potential target for antiviral development. *Antiviral Res* 178:104792. <https://doi.org/10.1016/j.antiviral.2020.104792>.
- Ghosh S, Dellibovi-Ragheb TA, Kerviel A, Pak E, Qiu Q, Fisher M, Takvorian PM, Bleck C, Hsu VW, Fehr AR, Perlman S, Achar SR, Straus MR, Whittaker GR, de Haan CAM, Kehrl J, Altan-Bonnet G, Altan-Bonnet N. 2020. Beta-coronaviruses use lysosomes for egress instead of the biosynthetic secretory pathway. *Cell* 183:1520–1535.e14. <https://doi.org/10.1016/j.cell.2020.10.039>.
- Komander D, Rape M. 2012. The ubiquitin code. *Annu Rev Biochem* 81:203–229. <https://doi.org/10.1146/annurev-biochem-060310-170328>.
- Bauer J, Bakke O, Morth JP. 2017. Overview of the membrane-associated RING-CH (MARCH) E3 ligase family. *N Biotechnol* 38:7–15. <https://doi.org/10.1016/j.nbt.2016.12.002>.
- Bartee E, Mansouri M, Hovey Nerenberg BT, Gouveia K, Fruh K. 2004. Downregulation of major histocompatibility complex class I by human ubiquitin ligases related to viral immune evasion proteins. *J Virol* 78:1109–1120. <https://doi.org/10.1128/jvi.78.3.1109-1120.2004>.
- Goto E, Ishido S, Sato Y, Ohgimoto S, Ohgimoto K, Nagano-Fujii M, Hotta H. 2003. c-MIR, a human E3 ubiquitin ligase, is a functional homolog of herpesvirus proteins MIR1 and MIR2 and has similar activity. *J Biol Chem* 278:14657–14668. <https://doi.org/10.1074/jbc.M211285200>.
- Ishido S, Wang C, Lee BS, Cohen GB, Jung JU. 2000. Downregulation of major histocompatibility complex class I molecules by Kaposi's sarcoma-associated herpesvirus K3 and K5 proteins. *J Virol* 74:5300–5309. <https://doi.org/10.1128/jvi.74.11.5300-5309.2000>.
- Coscoy L, Ganem D. 2000. Kaposi's sarcoma-associated herpesvirus encodes two proteins that block cell surface display of MHC class I chains by enhancing their endocytosis. *Proc Natl Acad Sci U S A* 97:8051–8056. <https://doi.org/10.1073/pnas.140129797>.
- Nash K, Chen W, Salganik M, Muzyczka N. 2009. Identification of cellular proteins that interact with the adeno-associated virus rep protein. *J Virol* 83:454–469. <https://doi.org/10.1128/JVI.01939-08>.
- Oh J, Shin JS. 2015. Molecular mechanism and cellular function of MHCII ubiquitination. *Immunol Rev* 266:134–144. <https://doi.org/10.1111/imr.12303>.
- Fujita H, Iwabu Y, Tokunaga K, Tanaka Y. 2013. Membrane-associated RING-CH (MARCH) 8 mediates the ubiquitination and lysosomal degradation of the transferrin receptor. *J Cell Sci* 126:2798–2809. <https://doi.org/10.1242/jcs.119909>.
- van de Kooij B, Verbrugge I, de Vries E, Gijzen M, Montserrat V, Maas C, Neeffjes J, Borst J. 2013. Ubiquitination by the membrane-associated RING-CH-8 (MARCH-8) ligase controls steady-state cell surface expression of tumor necrosis factor-related apoptosis inducing ligand (TRAIL) receptor 1. *J Biol Chem* 288:6617–6628. <https://doi.org/10.1074/jbc.M112.448209>.
- Bartee E, Eyster CA, Viswanathan K, Mansouri M, Donaldson JG, Fruh K. 2010. Membrane-associated RING-CH proteins associate with Bap31 and target CD81 and CD44 to lysosomes. *PLoS One* 5:e15132. <https://doi.org/10.1371/journal.pone.0015132>.
- Chen R, Li M, Zhang Y, Zhou Q, Shu HB. 2012. The E3 ubiquitin ligase MARCH8 negatively regulates IL-1 β -induced NF- κ B activation by targeting the IL1RAP coreceptor for ubiquitination and degradation. *Proc Natl Acad Sci U S A* 109:14128–14133. <https://doi.org/10.1073/pnas.1205246109>.
- Eyster CA, Cole NB, Petersen S, Viswanathan K, Fruh K, Donaldson JG. 2011. MARCH ubiquitin ligases alter the itinerary of clathrin-independent cargo from recycling to degradation. *Mol Biol Cell* 22:3218–3230. <https://doi.org/10.1091/mbc.E10-11-0874>.
- Roy N, Pacini G, Berlioz-Torrent C, Janvier K. 2017. Characterization of E3 ligases involved in lysosomal sorting of the HIV-1 restriction factor BST2. *J Cell Sci* 130:1596–1611. <https://doi.org/10.1242/jcs.195412>.
- Hewitt EW, Duncan L, Mufti D, Baker J, Stevenson PG, Lehner PJ. 2002. Ubiquitylation of MHC class I by the K3 viral protein signals internalization and TSG101-dependent degradation. *EMBO J* 21:2418–2429. <https://doi.org/10.1093/emboj/21.10.2418>.
- Mansouri M, Bartee E, Gouveia K, Hovey Nerenberg BT, Barrett J, Thomas L, Thomas G, McFadden G, Fruh K. 2003. The PHD/LAP-domain protein M153R of myxomavirus is a ubiquitin ligase that induces the rapid internalization and lysosomal destruction of CD4. *J Virol* 77:1427–1440. <https://doi.org/10.1128/jvi.77.2.1427-1440.2003>.

33. Coscoy L, Ganem D. 2001. A viral protein that selectively downregulates ICAM-1 and B7-2 and modulates T cell costimulation. *J Clin Invest* 107:1599–1606. <https://doi.org/10.1172/JCI12432>.
34. Boname JM, Stevenson PG. 2001. MHC class I ubiquitination by a viral PHD/LAP finger protein. *Immunity* 15:627–636. [https://doi.org/10.1016/S1074-7613\(01\)00213-8](https://doi.org/10.1016/S1074-7613(01)00213-8).
35. Cadwell K, Coscoy L. 2005. Ubiquitination on nonlysine residues by a viral E3 ubiquitin ligase. *Science* 309:127–130. <https://doi.org/10.1126/science.1110340>.
36. Cadwell K, Coscoy L. 2008. The specificities of Kaposi's sarcoma-associated herpesvirus-encoded E3 ubiquitin ligases are determined by the positions of lysine or cysteine residues within the intracytoplasmic domains of their targets. *J Virol* 82:4184–4189. <https://doi.org/10.1128/JVI.02264-07>.
37. Wang X, Herr RA, Chua WJ, Lybarger L, Wiertz EJ, Hansen TH. 2007. Ubiquitination of serine, threonine, or lysine residues on the cytoplasmic tail can induce ERAD of MHC-I by viral E3 ligase mK3. *J Cell Biol* 177:613–624. <https://doi.org/10.1083/jcb.200611063>.
38. Liu L, Oliveira NM, Cheney KM, Pade C, Dreja H, Bergin AM, Borgdorff V, Beach DH, Bishop CL, Dittmar MT, McKnight A. 2011. A whole genome screen for HIV restriction factors. *Retrovirology* 8:94. <https://doi.org/10.1186/1742-4690-8-94>.
39. Volchkov VE, Feldmann H, Volchkova VA, Klenk HD. 1998. Processing of the Ebola virus glycoprotein by the proprotein convertase furin. *Proc Natl Acad Sci U S A* 95:5762–5767. <https://doi.org/10.1073/pnas.95.10.5762>.
40. Coutard B, Valle C, de Lamballerie X, Canard B, Seidah NG, Decroly E. 2020. The spike glycoprotein of the new coronavirus 2019-nCoV contains a furin-like cleavage site absent in CoV of the same clade. *Antiviral Res* 176:104742. <https://doi.org/10.1016/j.antiviral.2020.104742>.
41. Checkley MA, Luttge BG, Freed EO. 2011. HIV-1 envelope glycoprotein biosynthesis, trafficking, and incorporation. *J Mol Biol* 410:582–608. <https://doi.org/10.1016/j.jmb.2011.04.042>.
42. Freed EO, Martin MA. 1995. The role of human immunodeficiency virus type 1 envelope glycoproteins in virus infection. *J Biol Chem* 270:23883–23886. <https://doi.org/10.1074/jbc.270.41.23883>.
43. Freed EO, Martin MA. 1996. Domains of the human immunodeficiency virus type 1 matrix and gp41 cytoplasmic tail required for envelope incorporation into virions. *J Virol* 70:341–351. <https://doi.org/10.1128/JVI.70.1.341-351.1996>.
44. Willey RL, Smith DH, Lasky LA, Theodore TS, Earl PL, Moss B, Capon DJ, Martin MA. 1988. In vitro mutagenesis identifies a region within the envelope gene of the human immunodeficiency virus that is critical for infectivity. *J Virol* 62:139–147. <https://doi.org/10.1128/JVI.62.1.139-147.1988>.
45. Dodd RB, Allen MD, Brown SE, Sanderson CM, Duncan LM, Lehner PJ, Bycroft M, Read RJ. 2004. Solution structure of the Kaposi's sarcoma-associated herpesvirus K3 N-terminal domain reveals a novel E2-binding C4HC3-type RING domain. *J Biol Chem* 279:53840–53847. <https://doi.org/10.1074/jbc.M409662200>.
46. Jabbour M, Campbell EM, Fares H, Lybarger L. 2009. Discrete domains of MARCH1 mediate its localization, functional interactions, and posttranscriptional control of expression. *J Immunol* 183:6500–6512. <https://doi.org/10.4049/jimmunol.0901521>.
47. Tran EE, Simmons JA, Bartesaghi A, Shoemaker CJ, Nelson E, White JM, Subramaniam S. 2014. Spatial localization of the Ebola virus glycoprotein mucin-like domain determined by cryo-electron tomography. *J Virol* 88:10958–10962. <https://doi.org/10.1128/JVI.00870-14>.
48. Ou X, Liu Y, Lei X, Li P, Mi D, Ren L, Guo L, Guo R, Chen T, Hu J, Xiang Z, Mu Z, Chen X, Chen J, Hu K, Jin Q, Wang J, Qian Z. 2020. Characterization of spike glycoprotein of SARS-CoV-2 on virus entry and its immune cross-reactivity with SARS-CoV. *Nat Commun* 11:1620. <https://doi.org/10.1038/s41467-020-15562-9>.
49. Ujike M, Huang C, Shirato K, Makino S, Taguchi F. 2016. The contribution of the cytoplasmic retrieval signal of severe acute respiratory syndrome coronavirus to intracellular accumulation of S proteins and incorporation of S protein into virus-like particles. *J Gen Virol* 97:1853–1864. <https://doi.org/10.1099/jgv.0.000494>.
50. Lontok E, Corse E, Machamer CE. 2004. Intracellular targeting signals contribute to localization of coronavirus spike proteins near the virus assembly site. *J Virol* 78:5913–5922. <https://doi.org/10.1128/JVI.78.11.5913-5922.2004>.
51. Samji T, Hong S, Means RE. 2014. The membrane associated RING-CH proteins: a family of E3 ligases with diverse roles through the cell. *Int Sch Res Notices* 2014:637295. <https://doi.org/10.1155/2014/637295>.
52. Schneider WM, Chevillotte MD, Rice CM. 2014. Interferon-stimulated genes: a complex web of host defenses. *Annu Rev Immunol* 32:513–545. <https://doi.org/10.1146/annurev-immunol-032713-120231>.
53. Colomer-Lluch M, Ruiz A, Moris A, Prado JG. 2018. Restriction factors: from intrinsic viral restriction to shaping cellular immunity against HIV-1. *Front Immunol* 9:2876. <https://doi.org/10.3389/fimmu.2018.02876>.
54. Schoggins JW, Rice CM. 2011. Interferon-stimulated genes and their antiviral effector functions. *Curr Opin Virol* 1:519–525. <https://doi.org/10.1016/j.coviro.2011.10.008>.
55. Zhang Y, Tada T, Ozono S, Kishigami S, Fujita H, Tokunaga K. 2020. MARCH8 inhibits viral infection by two different mechanisms. *Elife* 9:e57763. <https://doi.org/10.7554/eLife.57763>.
56. Nakamura N, Fukuda H, Kato A, Hirose S. 2005. MARCH-II is a syntaxin-6-binding protein involved in endosomal trafficking. *Mol Biol Cell* 16:1696–1710. <https://doi.org/10.1091/mbc.e04-03-0216>.
57. Nakamura N. 2011. The role of the transmembrane RING finger proteins in cellular and organelle function. *Membranes (Basel)* 1:354–393. <https://doi.org/10.3390/membranes1040354>.
58. Herr RA, Harris J, Fang S, Wang X, Hansen TH. 2009. Role of the RING-CH domain of viral ligase mK3 in ubiquitination of non-lysine and lysine MHC I residues. *Traffic* 10:1301–1317. <https://doi.org/10.1111/j.1600-0854.2009.00946.x>.
59. Yu C, Li S, Zhang X, Khan I, Ahmad I, Zhou Y, Li S, Shi J, Wang Y, Zheng YH. 2020. MARCH8 inhibits Ebola virus glycoprotein, human immunodeficiency virus type 1 envelope glycoprotein, and avian influenza virus H5N1 hemagglutinin maturation. *mBio* 11:e01882-20. <https://doi.org/10.1128/mBio.01882-20>.
60. Freed EO, Martin MA. 2013. Human immunodeficiency viruses: replication, p 1502–2456. *In* Knipe DM, Howley P (ed), *Fields virology*, 6th ed. Wolters Kluwer, Philadelphia, PA.
61. Feldmann H, Sanchez AS, Geisbert TW. 2013. Filoviridae: Marburg and Ebola viruses, p 923–2456. *In* Knipe DM, Howley P (ed), *Fields virology*, 6th ed. Wolters Kluwer, Philadelphia, PA.
62. Masters PS, Perlman S. 2013. Coronaviridae, p 825–2456. *In* Knipe DM, Howley P (ed), *Fields virology*, 6th ed. Wolters Kluwer, Philadelphia, PA.
63. Lyles DS, Kuzmin IV, Rupprecht CE. 2013. Rhabdoviridae, p 885–2456. *In* Knipe DM, Howley P (ed), *Fields virology*, 6th ed. Wolters Kluwer, Philadelphia, PA.
64. Sa Ribero M, Jouvenet N, Dreux M, Nisole S. 2020. Interplay between SARS-CoV-2 and the type I interferon response. *PLoS Pathog* 16:e1008737. <https://doi.org/10.1371/journal.ppat.1008737>.
65. Acosta PL, Byrne AB, Hijano DR, Talarico LB. 2020. Human type I interferon antiviral effects in respiratory and reemerging viral infections. *J Immunol Res* 2020:1372494. <https://doi.org/10.1155/2020/1372494>.
66. Zhang Q, Bastard P, Liu Z, Le Pen J, Moncada-Velez M, Chen J, Ogishi M, Sabli IKD, Hodeib S, Korol C, Rosain J, Bilguvar K, Ye J, Bolze A, Bigio B, Yang R, Arias AA, Zhou Q, Zhang Y, Onodi F, Korniotis S, Karpf L, Philippot Q, Chbihi M, Bonnet-Madin L, Dorgham K, Smith N, Schneider WM, Razoogy BS, Hoffmann H-H, Michailidis E, Moens L, Han JE, Lorenzo L, Bizien L, Meade P, Neehus A-L, Ugurbil AC, Corneau A, Kerner G, Zhang P, Rapaport F, Seeleuthner Y, Manry J, Masson C, Schmitt Y, Schlüter A, Le Voyer T, Khan T, Li J, et al. 2020. Inborn errors of type I IFN immunity in patients with life-threatening COVID-19. *Science* 370:eabd4570. <https://doi.org/10.1126/science.abd4570>.
67. Gale M, Jr, Sen GC. 2009. Viral evasion of the interferon system. *J Interferon Cytokine Res* 29:475–476. <https://doi.org/10.1089/jir.2009.0078>.
68. Murakami T, Freed EO. 2000. The long cytoplasmic tail of gp41 is required in a cell type-dependent manner for HIV-1 envelope glycoprotein incorporation into virions. *Proc Natl Acad Sci U S A* 97:343–348. <https://doi.org/10.1073/pnas.97.1.343>.
69. Freed EO, Martin MA. 1995. Virion incorporation of envelope glycoproteins with long but not short cytoplasmic tails is blocked by specific, single amino acid substitutions in the human immunodeficiency virus type 1 matrix. *J Virol* 69:1984–1989. <https://doi.org/10.1128/JVI.69.3.1984-1989.1995>.
70. Yee JK, Friedmann T, Burns JC. 1994. Generation of high-titer pseudotyped retroviral vectors with very broad host range. *Methods Cell Biol* 43(Pt A):99–112. [https://doi.org/10.1016/S0091-679X\(08\)60600-7](https://doi.org/10.1016/S0091-679X(08)60600-7).
71. Burns JC, Friedmann T, Driever W, Burrascano M, Yee JK. 1993. Vesicular stomatitis virus G glycoprotein pseudotyped retroviral vectors: concentration to very high titer and efficient gene transfer into mammalian and nonmammalian cells. *Proc Natl Acad Sci U S A* 90:8033–8037. <https://doi.org/10.1073/pnas.90.17.8033>.

72. Sherer NM, Lehmann MJ, Jimenez-Soto LF, Ingmundson A, Horner SM, Cicchetti G, Allen PG, Pypaert M, Cunningham JM, Mothes W. 2003. Visualization of retroviral replication in living cells reveals budding into multivesicular bodies. *Traffic* 4:785–801. <https://doi.org/10.1034/j.1600-0854.2003.00135.x>.
73. Platt EJ, Wehrly K, Kuhmann SE, Chesebro B, Kabat D. 1998. Effects of CCR5 and CD4 cell surface concentrations on infections by macrophagetropic isolates of human immunodeficiency virus type 1. *J Virol* 72:2855–2864. <https://doi.org/10.1128/JVI.72.4.2855-2864.1998>.
74. Wei X, Decker JM, Liu H, Zhang Z, Arani RB, Kilby JM, Saag MS, Wu X, Shaw GM, Kappes JC. 2002. Emergence of resistant human immunodeficiency virus type 1 in patients receiving fusion inhibitor (T-20) monotherapy. *Antimicrob Agents Chemother* 46:1896–1905. <https://doi.org/10.1128/aac.46.6.1896-1905.2002>.
75. Stauffer W, Sheng H, Lim HN. 2018. EzColocalization: an ImageJ plugin for visualizing and measuring colocalization in cells and organisms. *Sci Rep* 8:15764. <https://doi.org/10.1038/s41598-018-33592-8>.